Van der Meer Consulting B.V.
COASTAL ENGINEERING CONSULTANCY & RESEARCH

# The Wave Run-up Simulator

## Idea, necessity, theoretical background and design

**Project number:** vdm11355

**Version:** 1.1

**Date:** 12 February 2011

# Samenvatting

Het idee van de Golfoploopsimulator is gebaseerd op de ervaringen met de Golfoverslagsimulator. Het is mogelijk gebleken om golftongen die over een kruin van een dijk slaan in werkelijkheid te simuleren. Het moet ook mogelijk zijn de golven in de golfoploop- en neerloop zone te simuleren. Dit is de zone *nadat* de golven zijn gebroken en het talud op lopen.

Dit rapport beschrijft het idee van de Golfoploopsimulator, waarom het nuttig is om deze machine te ontwikkelen, er onderzoek mee te doen en een toetsmethode af te leiden. In feite kan de toetsmethode al worden afgeleid van de cumulatieve overbelastingsmethode, die voor golfoverslag is ontwikkeld. Het betekent dat proeven dan uitsluitend hoeven te worden gedaan ter validatie van de voorspellingsmethode. Het tweede deel van het rapport beschrijft in detail wat er bekend is over de golfbeweging in de oploopzone en wat dus de Golfoploopsimulator zou moeten simuleren.

**Hoofdstuk 1** geeft een korte samenvatting van wat de Golfoverslagsimulator is en hoe op basis van de ervaring van vier jaar onderzoek het mogelijk moet zijn een Golfoploopsimulator te ontwikkelen.

De eerste vraag is of er wel een Golfoploopsimulator moet komen en of het wel zinnig is onderzoek uit te voeren op het zeewaartse talud van dijken. In **hoofdstuk 2** wordt een groot aantal voorbeelden gegeven van zee- en meerdijken en het blijkt dat het overgrote deel van de Nederlandse zee- en meerdijken een boventalud hebben dat bedekt is met gras. Dit is altijd in de oploopzone, met een enkele uitzondering. Er is geen gevalideerde toetsmethode voor de sterkte van boventaluds van gras. Het probleem is niet aanwezig bij rivierdijken, waar de golven vaak klein zijn en ook de golfklapzone met gras is bedekt. Er is onderzoek uitgevoerd naar de sterkte van dit soort grastaluds onder golfaanval, waarbij de golfhoogte beperkt is. Als de klapzone sterk genoeg is, is ook de oploopzone sterk genoeg. Het probleem speelt dus vooral bij zee- en meerdijken.

Toen de Golfoverslagsimulator werd ontwikkeld, was er weinig bekend over sterkte van binnentaluds van dijken bij golfoverslag. De eerste jaren van onderzoek waren dan ook bedoeld om inzicht en ervaring te krijgen wat golfoverslag doet en hoe schade ontstaat en zich ontwikkelt. Pas vorig jaar is een methode ontwikkeld die veel potentie heeft om een goede predictiemethode te worden. **Hoofdstuk 3** beschrijft samenvattend wat de resultaten zijn met de Golfoverslagsimulator en hoe de predictiemethode, de cumulatieve overbelastingsmethode, eruit ziet en ook hoe deze vrij eenvoudig in een gedetailleerde toetsing kan worden toegepast. De methode gaat uit van een sterkteparameter voor het gras, beschreven door een kritieke snelheid, en van de snelheid die elke overslaande golf teweeg brengt.

Aangezien ook in de oploopzone het gaat om de snelheid van de op- en neer lopende golf, kan de methode direct worden uitgebreid naar de oploopzone. Dit houdt ook in dat eventuele proeven op het buitentalud van zee- en meerdijken uitsluitend zijn bedoeld ter validatie van een predictiemethode.

De snelheden, oploophoogten en laagdikten over het hele talud in de oploopzone moeten goed bekend zijn om een goede simulatie uit te voeren. Hier is wel onderzoek naar gedaan, maar nooit met het oogmerk om een Golfoploopsimulator te ontwerpen. Daarom is in **hoofdstukken 4 en 5** een gedetailleerde analyse uitgevoerd naar wat uit de literatuur bekend is en wat uit bestaande metingen kan worden gehaald. In **hoofdstuk 4** wordt voornamelijk naar metingen gekeken die zijn uitgevoerd op de buitenkruinlijn en die deels ook zijn gebruikt bij de ontwikkelingen van de Golfoverslagsimulator. De beschrijvingen van snelheid en laagdikte zijn niet altijd eensluidend.

Een andere methode, welke in **hoofdstuk 5** is uitgewerkt, is om te kijken naar het signaal van golfoploopmetingen. De afgeleide van de plaats van het front van de oplopende golf geeft namelijk de snelheid op het talud en wel over het hele talud, niet op een vaste locatie. Het blijkt dat de snelheid van de oplopende golftong *niet* lineair afneemt met de hoogte op het talud, maar dat vrijwel vanaf het begin van de oploop tot vrijwel een niveau van driekwart van de uiteindelijke oploophoogte de snelheid hoog is en dichtbij de maximum snelheid. Pas in het hoogste kwart van de oploop neemt de snelheid sterk af.

Deze bevinding komt ook terug in de uiteindelijke beschrijving van de snelheden op het talud. Er is wel een gemiddelde trend dat de snelheden toenemen bij toenemende oploopniveaus, maar er komen veel snelheden voor bij eenzelfde oploopniveau. Dit is een beetje vergelijkbaar met golven: er komen verschillende golfperioden voor bij individuele golven die vrijwel dezelfde hoogte hebben. Zowel de golfhoogte als de golfperiode hebben een specifieke verdeling en zijn niet direct aan elkaar gekoppeld. Een simulatie van golfoploop moet dan ook bestaan uit het simuleren van verschillende snelheden, terwijl wel een vrijwel identiek oploopniveau wordt bereikt.

Het laatste **hoofdstuk 6** geeft een samenvatting van de oploopcondities die moeten worden gesimuleerd. Daarnaast worden oplossingen voorgesteld om van de bestaande Golfoverslagsimulator uit te gaan en enkele aanpassingen te plegen. Een daarvan is om de klepopening onderdeel te maken van de sturing. Deze methode is al ontwikkeld voor de Gofloverslagsimulator in de VS. Hiermee zou, samen met een specifiek volume, een verband gesimuleerd kunnen worden tussen snelheid en oploophoogte en dus ook de simulatie van verschillende snelheden bij dezelfde oploophoogten (door het volume, als ook de klepstand, te veranderen). Tenslotte moet de overgangsconstructie zo gemaakt worden dat het mogelijk is het terugkomende water kwijt te raken voordat de volgende oplopende golf wordt gesimuleerd.

Samenvattend kan worden geconcludeerd dat het niet al te moeilijk moet zijn om een Golfoploopsimulator te ontwikkelen. Grastaluds in de oploopzone komen veelvuldig voor op zee- en meerdijken en er is geen gevalideerde toetsmethode. De recent ontwikkelde predictiemethode voor golfoverslag kan rechtstreeks worden omgebouwd naar een predictiemethode voor het zeewaartse deel in de oploopzone. Eventuele proeven zijn dan vooral bedoeld om deze methode te valideren. Daarmee kan met een Golfoploopsimulator worden voortgebouwd op het werk van de Golfoverslagsimulator en zijn de inspanningen om te komen tot een goede toetsmethode voor grastaluds in de oploopzone aanzienlijk beperkter dan wat tot nu toe met de Golfoverslagsimulator is uitgevoerd en nog zal worden uitgevoerd.

Geschreven door: dr ir J.W. van der Meer

Van der Meer Consulting B.V.
COASTAL ENGINEERING CONSULTANCY & RESEARCH

P.O. Box 423
8440 AK Heerenveen
The Netherlands
Tel. +31 651574953
jm@vandermeerconsulting.nl
www.vandermeerconsulting.nl

# Executive summary

The idea of the Wave Run-up Simulator is based on the experiences with the Wave Overtopping Simulator. It is possible to simulate wave tongues overtopping a dike crest in reality. It must also be possible to simulate waves in the run-up and run-down zone of the seaward slope. This is the zone after waves have broken and when they rush-up the slope.

The present report describes the idea of the Wave Run-up Simulator, why it is useful to develop the machine, to perform research with it and to develop a prediction method for slope strength. In fact, a prediction method can already be developed from the cumulative overload method, which was developed on the basis of results with the Wave Overtopping Simulator. It also means that tests on the seaward slope will be done for validation purposes only. The second part of the report describes in detail what is known about the movement of waves in this run-up zone and what actually the Wave Run-up Simulator has to simulate.

**Chapter 1** gives a short summary of the Wave Overtopping Simulator and how it should be possible to develop a Wave Run-up Simulator on the basis of four years of research with the Wave Overtopping Simulator.

The first question is whether it is useful to develop and construct a Wave Run-up Simulator to look at strength of seaward slopes with grass coverage. **Chapter 2** gives a large number of examples of existing sea and lake dikes in the Netherlands. It is concluded that the majority of these dikes have a run-up zone at the seaward side which is covered with grass. Right now no validated safety assessment method exists for these kind of slopes. The problem does not exist for river dikes, where the waves are small and where often the impact zone is also covered by grass. Research has been performed for this kind of circumstances and safety assessment methods exist. If the impact zone can resist the wave attack, the run-up zone will then certainly be able to do this. The problem exists only for sea and lake dikes.

At the time the Wave Overtopping Simulator was developed hardly anything was known about the strength of grass covered slopes against wave overtopping. The first years of research were mainly observation tests to get insight in how damage was created and developed. Only recently a method was developed with the potential of becoming a reliable prediction method. **Chapter 3** gives a summary of the results with the Wave Overtopping Simulator and the prediction method, the cumulative overload method, how it works and how a fairly easy application of a safety assessment method looks like. The method includes a strength parameter for the grass, given by a critical velocity, and the velocity of each overtopping wave.

Waves in the run-up zone have also a certain velocity along the slope, upwards and downwards. This means that in principle the cumulative overload method can also be applied in the run-up zone. Possible tests with the Wave Run-up Simulator then will be used to validate this method, rather than starting from scratch.

Flow velocities, run-up levels and flow depths must be known over the full run-up zone in order to make a good simulation. Some research has been performed, but never with the objective to design a Wave Run-up Simulator. For this reason a detailed analysis has been performed in **Chapters 4 and 5** on what is known in literature and on analysis of existing data from tests. **Chapter 4** describes measurements performed at the crest of dikes, which have partly been used to develop the Wave Overtopping Simulator. Descriptions do not always lead to similar conclusions.

Another method, described in **Chapter 5**, is to look at the records of wave run-up gauges. The derivative of the location of the up-rushing wave front gives the front velocity over the full run-up zone, not only at a fixed position. It appears that the velocity along the slope does *not* linearly decrease with the run-up level. Almost from the start of run-up to about three quarters of the maximum run-up level the flow velocity is high and close to the maximum velocity. The velocity decreases suddenly in the last quarter of the run-up.

This conclusion returns in the final description of flow velocities in the run-up zone. An average trend exists that flow velocity increases with increasing maximum run-up level, but a large range of flow velocities exist for similar run-up levels. This is more or less similar to waves: various wave periods exist for similar individual wave heights. Wave height as well as wave periods have both a certain distribution and are not directly correlated by an equation. The simulation of up-rushing waves in the run-up zone must exist of the simulation of different flow velocities, whilst a similar maximum run-up has to be reached.

The final **Chapter 6** gives a summary of the run-up conditions, like flow velocity and maximum run-up level, that has to be simulated. Solutions are proposed how to modify the existing Wave Overtopping Simulator in such a way that it can also simulate run-up. One solution is to make the opening of the valve part of the steering of the Simulator. This method has already been developed for the Wave Overtopping Simulator in the US. Released volume and opening of the valve will give a relationship with run-up velocity and maximum run-up level. In this way it must be possible to simulate different flow velocities for similar maximum run-up levels. Finally, the transition from the water containing box to the slope has to be modified in such a way that down-rushing water is able to be released before the next up-rushing wave will be simulated.

In summary one may conclude that it will not be too difficult to develop a Wave Run-up Simulator. Grass covered slopes on the seaward slopes of dikes, in the run-up zone, do exist on many of the sea and lake dikes in the Netherlands and no validated safety assessment method exists. The recently developed safety assessment method for wave overtopping can be modified to a safety assessment method for the run-up zone. Possible tests then have the objective of validation, rather than starting from scratch. The Wave Run-up Simulator is then a logical continuation of the Wave Overtopping Simulator. Efforts to come to a good safety assessment method for grass covered slopes in the run-up zone will therefore be significantly smaller than the research that has been performed, and still will be performed, with the Wave Overtopping Simulator.

Performed by: Dr. J.W. van der Meer

**Van der Meer Consulting B.V.**
*COASTAL ENGINEERING CONSULTANCY & RESEARCH*

P.O. Box 423
8440 AK Heerenveen
The Netherlands
Tel. +31 651574953
jm@vandermeerconsulting.nl
www.vandermeerconsulting.nl

# Contents

# 1 Introduction to the new invention

## 1.1 General

The idea to develop a Wave Run-up Simulator is of course based on the experience with the Wave Overtopping Simulator. After four years of extensive testing and very recently the development of a prediction method, further testing with the Wave Overtopping Simulator will be focused on validation of the prediction method and testing of river dikes and possibly regional dikes, which have quite different features than sea and lake dikes. The objective of the Wave Overtopping Simulator is to simulate the hydraulic behaviour of wave overtopping on real dikes and to observe the damage development of grassed slopes, leading to a prediction method for strength of dikes due to wave overtopping.

The Wave Overtopping Simulator simulates overtopping wave tongues on crest and landward slope dikes. Waves that reach the crest in real situations are simulated, not the wave breaking and wave run-up or run-down on the seaward side. The idea of the Wave Run-up Simulator is to simulate the wave run-up and run-down on the seaward side, but above the zone of breaking waves. Many sea and lake dikes exist in the Netherlands, where the impact zone of waves is protected by block revetments or asphalt, but the most upper part of the seaward side consists of grass only.

The developed prediction method (cumulative overload method) is also a first step for a prediction method for strength of grassed slopes in the run-up and run-down zone. But now the water runs up a slope and then, if there is no or hardly overtopping, will run-down till the next up-rushing wave arrives. With wave overtopping there is a relationship between overtopping wave volume and flow velocity and flow depth. This is not the case for wave run-up, where flow velocities and flow depths are the direct input for simulation.

The main similarity, however, is that the cumulative overload method is based on flow velocities and quality of the grass cover. A good description of the velocities in the run-up and run-down zone gives an initial prediction method for the strength of this zone. This is in contrast with the development of the Wave Overtopping Simulator, where first years of testing was based on gathering knowledge and then developing a prediction method.

A prediction method for strength of grass covers in the run-up and run-down zone can already be developed. The objective of the Wave Run-up Simulator is then to *validate* this method in real situations.

The copy right of the idea of the Wave Run-up Simulator is based on the submission of a research topic to the ENW research agenda on 13 December 2010.

The idea of the Wave Overtopping Simulator has shortly been summarized in Section 1.2. The idea of the Wave Run-up Simulator has been elaborated in Section 1.3 and the conclusion has been reached that wave run-up simulation is only important for sea and lake dikes, not for river dikes and other dikes where only small wave attack is possible and where often the impact zone of waves has also a grass cover.

Chapter 2 focuses on the actual situation in the Netherlands. Do we indeed have dikes with only grass cover in the run-up and run-down zone? Is this only for a few kilometers of dike or is it the main situation?

We do not have to start from scratch like in 2006 for the Wave Overtopping Simulator. It is possible to build on results and developed theory in the past four years of research with the Wave Overtopping Simulator. Chapter 3 shortly summarizes the re-

sults and the recently developed prediction method, including the way to come to a prediction method for the seaward side.

The Wave Overtopping Simulator was developed based on theory of individual overtopping wave volumes and associated flow velocities at the crest. This cannot be used for the Wave Run-up Simulator, where flow velocities and flow depths change along the slope. What are the theoretical boundary conditions for design of a Wave Run-up Simulator? Chapter 4 gives an analysis of existing literature on a direct measurement of flow depth and velocity, which is mainly based on the seaward crest and not on the run-up zone. Chapter 5 focuses on analysis of the flow velocity in the run-up zone, based on records of a wave run-up gauge. All this analysis leads to a description of flow velocities and flow depths in the run-up zone and are boundary conditions for the design of the Wave Run-up Simulator.

Finally, in Chapter 6 the design of the Wave Run-up Simulator is given. Questions solved are:

- How does a Wave Run-up Simulator look like, can for instance the Wave Overtopping Simulator be modified?
- Water that runs down the slope meets the Simulator again and should be released before the next up-rushing wave is simulated. How can this be solved?
- The number of overtopping waves at the crest is limited and always smaller than the number of incident waves. But every wave runs up a slope. How can this be simulated?

## 1.2 Wave Overtopping Simulator

The Wave Overtopping Simulator has been designed and constructed in 2006 and has been used since then for destructive tests on dike crest and landward slopes of dikes or levees under loading of overtopping waves. The idea of the Wave Overtopping Simulator was quite simple: try to simulate the overtopping wave tongue on a dike crest, based on theory of flow velocity and flow depth of overtopping wave volumes. It is not required to simulate the real (breaking) waves, only the part of the wave that reaches the crest. The principal is shown in Figure 1,1, a setup of the real Overtopping Simulator in Figure 1.2.

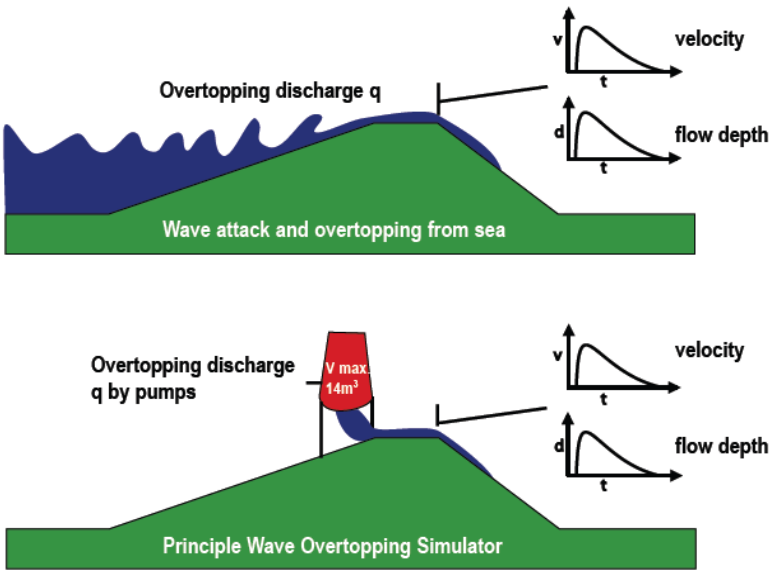


Figure 1.1. Principal of the Wave Overtopping Simulator.

Figure 1.2. Wave Overtopping Simulator on a real dike.


Figure 1.3. Release of a large overtopping wave volume.

Water is pumped into a box and released now and then through a butterfly valve, simulating an overtopping wave volume. Figure 1.3 shows the release of a large overtopping wave. Released volumes in a certain time are according to theoretical distributions of overtopping wave volumes, depending on assumed wave conditions at the sea side and assumed crest freeboard. The purpose of testing is to investigate the strength of crest and landward slopes of dikes due to wave overtopping and develop a prediction method.

## 1.3 The Wave Run-up Simulator

When incident waves reach a dike or levee, they will break if the slope is fairly gentle. This may cause impacts on the slope in zone 2, see Figure 1.4. When large waves attack such a dike the seaward side in this area will often be protected by a placed block revetment or asphalt. The reason is simple: grass covers cannot withstand large wave impacts, unless the slope is very mild.

Above the impact zone the wave runs up the slope and then rushes down the slope till it meets the next up-rushing wave. This is the run-up and run-down zone on the seaward slope (zone 3 in Figure 1.4). Up-rushing waves that reach the crest will overtop the structure and the flow is only to one side: down the landward slope. Zone's 4 and 5 can be tested with the Wave Overtopping Simulator, described in Section 1.2.

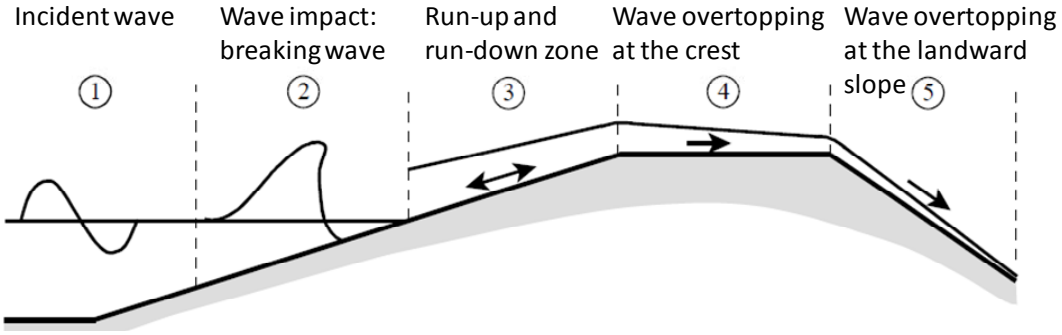


Figure 1.4. Process of wave breaking, run-up and overtopping at a dike (figure partly from Schüttrumpf, 2001).

The seaside of a grassed dike cannot be tested with the Wave Overtopping Simulator. Overtopping water is released from the Simulator and flows over the crest and down the landward slope. The flow of water is only down the landward slope and does not return to the Simulator. But this is the case at the seaward side in the run-up and run-down zone.

The objective of a Wave Run-up Simulator would be to test strength of grass slopes in the run-up and run-down zone at the seaward side.

The first question to answer is, do we need such a Run-up Simulator? It is clear that wave overtopping may give erosion to the landward side of any dike, whether it is a sea or lake dike with fairly severe wave attack or a river dike with relatively small overtopping waves. This situation is different when we consider a grassed seaward slope in the run-up and run-down zone.

When the wave attack is quite small, like for river dikes, the seaward side is often not protected by an artificial system and the grassed slope should also be able to withstand wave impacts (zone 2 in Figure 1.4) of these relatively small waves. Tests in wave flumes have shown that grassed slopes are indeed able to withstand small waves, say less than 1 m. If grassed slopes can withstand small wave impacts, then they are certainly able to withstand the lower forces in the wave run-up and run-down zone. The Wave Run-up Simulator cannot simulate wave impacts. And therefore there is no need for a Wave Run-up Simulator to test the seaward side if the impact zone is also protected by grass.

Many sea and lake dikes have artificial protection in the impact zone of the waves and above this zone, at the run-up and run-down zone, the slope is covered by grass. This upper part of the slope, often above a protected berm, gets only wave run-up and run-down and no wave impacts.

Wave run-up at these upper seaward slopes may give larger velocities than at the crest and landward slope during wave overtopping. And the grass is attacked by two sides, from up-rushing water and then by down-rushing water. The conclusion is that a grassed upper slope on the seaward side will experience larger forces by up and down rushing waves than the crest and landward slope by only down rushing waves.

There are many sea and lake dikes (in the Netherlands) with fairly large wave attack where the upper part of the seaward side has only a grass protection. Chapter 2 gives

an overall view of the situation in the Netherlands.

With all the experience gained from destructive tests on wave overtopping we cannot yet establish the strength of grassed seaward slopes in the wave run-up and run-down zone. This is the area where a Wave Run-up Simulator would be very useful. But we can make a prediction method first, based on the recently developed cumulative overload method for wave overtopping. Tests are then mainly performed to validate this method.

For the time being, the idea of a Wave Run-up Simulator is more or less similar to the Wave Overtopping Simulator. Differences are that not the volume of a wave is important, but more the correct velocity at the right location and that an up-rushing wave comes (partly) back to the Simulator. Another difference might be that not every wave can be simulated, although most waves will reach the upper slope.

# 2 Actual situation in the Netherlands

The idea is to test the grassed upper seaward slope of dikes with the Wave Run-up Simulator. But what are actual situations in the Netherlands? Are there many dikes with grassed upper slopes, what are the slope angles, is there a berm and at which level?

In order to get an idea a short inventory has been made. The first part consists of the seadikes where the landward side was tested with the Wave Overtopping Simulator. The second part shows a series of pictures of dikes along the Dutch sea or lake coasts.

Figure 2.1 shows the dike at Delfzijl, which has been tested with the Wave Overtopping Simulator in 2007. This stretch of dike is partly protected by the breakwaters of the Eemshaven and wave attack will be limited. The seaward side is a 1:3 slope with a berm and has a grass cover over the full length.

Figures 2.2 - 2.4 show the Waddensea dike at the Boonweg, the location that was tested in 2008. Figure 2.2 shows the view from the crest of the dike and indeed the seaward side has a grass cover on a slope of 1:5.2. The crest height is situated 8.9 m above design water level. Figure 2.3 is taken from the berm and shows the same 1:5.2 grassed slope, which turns into an open revetment (for grass growth) and then an asphalt berm. The berm (or gentle slope) has a slope of 1:7 and runs from 6.3 to 7.3 m +NAP, where the design water level is 4.9 m +NAP. This protected part is well above the design water level. With a design wave height of 1.9 m the transition from protected to grass cover is 0.7 $H_s$ above the design water level. Finally, the down slope of 1:4.2 has been protected by asphalt.

It can be concluded that the upper part of the seaward side, 0.7 $H_s$ above design water level, is situated in the run-up zone and might be attacked by a wave height of 1.9 m.

Figure 2.1. Delfzijl - Waddensea. Right side is the landward slope, about 1:3. Left the seaward slope with first a high foreshore, a grassed down slope, a grassed berm and a grassed upper slope. Slopes are about 1:3. This part of the dike is protected for waves to some extent by the breakwaters in front of the harbour.

Figure 2.2. Boonweg - Waddensea. View from the crest. Landward slope on the right side. Upper grassed seaward slope 1:5.2.

Figure 2.3. Boonweg - Waddensea. Seaward side, asphalt berm 1:7, open revetment 1:7 and 1:5.2 grassed upper slope. Berm between 6.3 and 7.3 +NAP.

Figure 2.4. Boonweg - Waddensea. Seaward side, asphalt down slope 1:4.2.

Figures 2.5 and 2.6 show the tested section of St Philipsland (2008). The dike is situated at the Eastern Scheldt. The slopes are 1:3.5 with a berm 1:20, which is 5.6 m long. The berm level is 5 m +NAP and the crest level 6.6 m +NAP. Both upper slope and berm have a grass cover. The down slope has been protected by asphalt. The design water level is 3.7 m +NAP and the design wave height 0.95 m. These waves will break at the down slope and both berm and upper slope are in the run-up zone.

Figure 2.5. St Philipsland - Eastern Scheldt. Seaward side, upper grassed slope 1:3.5 wih grassed berm 1:20.

Figure 2.6. St Philipsland - Eastern Scheldt. Seaward side, grassed berm 1:20 with protected down slope 1:3.5.

Figures 2.7 and 2.8 show the situation at Kattendijke, tested in 2008. Figure 2.7 shows a view on the seaward side with the Wave Overtopping Simulator, testing the landward side of the dike. Figure 2.8 shows the seaward side from the berm. The grassed upper slope has a slope of 1:3.5, a berm of 1:20 is situated at 4.85 +NAP and the down slope is 1:3.0. The crest level is 6.5 +NAP. The down slope and the lowest part of the berm are protected by asphalt. The second part of the berm has a grass cover. The design water level is 3.5 m +NAP with a wave height of 0.75 s. The grassed area is well within the run-up zone, not in the impacting zone.

Figure 2.7. Kattendijke - Eastern Scheldt. View on the seaward side, including the Wave Overtopping Simulator which is testing the landward side.

Figure 2.8. Kattendijke - Eastern Scheldt. Seaward side, protected down slope 1:3.5, berm 1:20 with foot or cycle path and partly grassed slope, upper grassed slope 1:3.0.

The Afsluitdijk was tested in 2009, but this dike has been protected up to the crest level, as there will be quite some wave overtopping under design conditions. The Vechtdijk near Zwolle was tested in 2010, but this is a river dike, which means grass cover over the whole seaward side with very limited wave attack.

Three of the five tested sections with the Wave Overtopping Simulator are situated at the sea coast and have a grass cover on in the run-up zone on the seaward side.

A full survey on dikes with grass covered slopes in the run-up zone in the Netherlands is not within the scope of this study. But the data base of pictures of dikes contains quite a number of dikes along the sea coast as well as along the coasts of the IJsselmeer and Markermeer, the two large lakes in the Netherlands. Cross-sections of the dikes are not directly available, but design conditions (or actually conditions for a safety assessment) for the sea dikes can be found in the Hydraulic Boundary Conditions 2006.

The next series of photo's are from the picture data base and the first part (Figures 2.9 - 2.18) shows dikes along the sea (North Sea, Waddensea, Eastern Scheldt), with the second part (Figures 2.19 - 2.24) dikes along IJsselmeer and Markermeer. All of them have an upper seaward slope covered with grass. The legends of the Figures give the location of the picture with design wave height and water level, if available.

The main conclusion is that many dikes exist in the Netherlands with a grass cover on the seaward side in the run-up zone. This part of the seaward side will certainly be attacked under design conditions, where wave overtopping could still be very limited.


Figure 2.9. Seadike Groningen with the Eemshotel. Design water level 5.9 m +NAP; design wave height 1.2 m.

Figure 2.10. Dike between Harlingen and Afsluitdijk. Design water level 5.0 m +NAP; design wave height 2.2 m.

Figure 2.11. Dike Breedbaerdtpolder, Groningen. Design water level 6.4 m +NAP; design wave height 1.4 m.

Figure 2.12. Dike near Wilhelmandorp, Zeeland. Design water level 3.5 m +NAP; design wave height 1.1 m.

Figure 2.13. Dike near Wemeldinghe, directly after renovation. Design water level 3.6 m +NAP; design wave height 0.9 m.

Figure 2.14. Dike at Maasvlakte I, facing the North Sea. At some locations bad grass coverage. Design water level about 5 m +NAP. Design wave height not available, but between 5-8 m.

Figure 2.15. Dike at Maasvlakte I, facing the North Sea. Here better grass coverage. Design water level about 5 m +NAP. Design wave height not available, but between 5-8 m.

Figure 2.16. Dike at Ameland. Protected slope below 2 m +NAP, then a cycling path as berm. Upper slope about 1:5. Design water level 4.5 m +NAP; design wave height 1.6 m.

Figure 2.17. Grassed upper slope of a dike at Groningen, damaged by the storm of 1 November 2006.

Figure 2.18. Grassed upper slope of a dike at Groningen with a transition. Grass damaged (left side of photo) and transition damaged by the storm of 1 November 2006.

Figure 2.19. Dike at Andijk along the IJsselmeer.

Figure 2.20. Dike along Flevoland near the power plant, facing the IJsselmeer.

Figure 2.21. North side of Houtribdijk, facing the IJsselmeer.

Figure 2.22. South side of Houtribdijk, facing the Markermeer.

Figure 2.23. Dike in Friesland, facing the IJsselmeer.

Figure 2.24. Wieringermeerdijk, facing the IJsselmeer.

# 3 Results and developed prediction method from overtopping

## 3.1 Results

First tests with the Wave Overtopping Simulator were performed in 2007 at the seadike at Delfzijl. At that time hardly anything was known about how a certain overtopping discharge would look like, for what discharges damage could be expected and how the damage would look like. The first tests were really observation tests.

Nevertheless, every time a test was scheduled, a prediction report was made. After testing the prediction was compared with the results in an evaluation report. Up to now, even after four years of extensive testing, hardly any prediction was close to what really occurred. This shows that it is not easy at all to come to a prediction method which can be validated by further testing, instead of going on with mainly observation tests. Recently, however, after the recent tests in 2010 at the Vechtdijk, a prediction method could be developed. It is this method that is also the starting point for a prediction method for erosion of the seaward slope in the run-up and run-down zone. This time we do not have to start from scratch, but a good prediction method can be developed beforehand and the tests can be used for validation.

This chapter summarizes first where the results of all the testing has been published. It will then describe a few main conclusions. The last part summarizes the developed prediction method for landward slopes under wave overtopping.

The first testing at Delfzijl was performed under the European program ComCoast and reports can be found on the website (www.comcoast.org). After the first series the research became part of the Research Project SBW (Strength and Loads on Water defences) of the Rijkswaterstaat. Each series of tests was documented (in Dutch) in four reports, covering prediction, testing, evaluation and model development. The following reports have been written:

Fase 1D Evaluatie Delfzijl
Fase 2A Modelontwikkeling Boonweg
Fase 2B Predictie Boonweg
Fase 2C Proefuitvoering Boonweg (factual report)
Fase 2D Evaluatie Boonweg
Fase 3A Modelontwikkeling Afsluitdijk
Fase 3B Predictie Afsluitdijk
Fase 3C Proefuitvoering Afsluitdijk (factual report)
Fase 3D Evaluatie Afsluitdijk
Fase 4A Modelontwikkeling Vechtdijk
Fase 4B Predictie Vechtdijk
Fase 4C Proefuitvoering Vechtdijk (factual report)
Fase 4D Evaluatie Vechtdijk
Fase 5C Proefuitvoering Zeeland (factual report St. Philipsland en Kattendijke)
Fase 5D Evaluatie Zeeland St. Philipsland en Kattendijke

Besides the Dutch reports many papers have been written for conferences. The following list gives these papers and most of them can be downloaded from the website (www.vandermeerconsulting.nl).

Van der Meer, J.W., P. Bernardini, W. Snijders and H.J. Regeling (2006). The wave overtopping simulator. *ASCE, ICCE 2006, San Diego, pp. 4654 - 4666*.

Van der Meer, J.W., P. Bernardini, G.J. Steendam, G.J. Akkerman and G.J.C.M. Hoffmans (2007). The wave overtopping simulator in action. *Proc. Coastal Structures, Venice, Italy.*

Akkerman, G.J., P. Bernardini, J.W. van der Meer, H. Verheij and A. van Hoven 2007). Field tests on sea defineces subject to wave overtopping. *Proc. Coastal Structures, Venice, Italy.*

Van der Meer, J.W., G.J. Steendam, G. de Raat and P. Bernardini (2008). Further developments on the wave overtopping simulator. *ASCE, Proc. ICCE 2008, Hamburg, 2957-2969.*

Steendam, G.J., W. de Vries, J.W. van der Meer, A. van Hoven, G. de Raat and J.Y. Frissel (2008). Influence of management and maintenance on erosive impact of wave overtopping on grass covered slopes of dikes; Tests. *Proc. FloodRisk, Oxford, UK. Flood Risk Management: Research and Practice – Samuels et al. (eds.) ISBN 978-0-415-48507-4; pp 523-533.*

Hoffmans, G., G.J. Akkerman, H. Verheij, A. van Hoven and J.W. van der Meer (2008). The erodibility of grassed inner dike slopes against wave overtopping. *ASCE, Proc. ICCE 2008, Hamburg, 3224-3236*.

Van der Meer, J.W., R. Schrijver, B. Hardeman, A. van Hoven, H. Verheij and G.J. Steendam (2009). Guidance on erosion resistance of inner slopes of dikes from three years of testing with the Wave Overtopping Simulator. *Proc. ICE, Coasts, Marine Structures and Breakwaters 2009, Edinburgh, UK.*

Van der Meer, J.W., B. Hardeman, G.J. Steendam, H. Schttrumpf and H. Verheij (2010). Flow depths and velocities at crest and inner slope of a dike, in theory and with the Wave Overtopping Simulator. *ASCE, Proc. ICCE 2010, Shanghai*.

Steendam, G.J., J.W. van der Meer, B. Hardeman and A. van Hoven (2010). Destructive wave overtopping tests on grass covered landward slopes of dikes and transitions to berms. *ASCE, Proc. ICCE 2010, Shanghai*.

Le Hai Trung, J.W. van der Meer, G.J. Schiereck, Vu Minh Cath and G. van der Meer (2010). Wave Overtopping Simulator Tests in Vietnam. ASCE, *Proc. ICCE 2010, Shanghai.*

Van Hoven, A., B. Hardeman, J.W. van der Meer and G.J. Steendam (2010). Sliding stability of landward slope clay cover layers of sea dikes subject to wave overtopping. *ASCE, Proc. ICCE 2010, Shanghai.*

Finally, an English summary report has been written about the results, observations and first conclusions after the first two years of testing. This report is also for download at the mentioned website.

## 3.2 Prediction method

The first three years of testing in the Netherlands with the Wave Overtopping Simulator was done for an assumed wave condition of $H_s$ = 2 m and $T_p$ = 5.7 s, being an average wave condition for the Dutch dikes. But estuaries, rivers and small lakes may have design conditions which are smaller, whereas dikes directly facing the North Sea may have larger conditions. It is the crest freeboard that governs the actual overtopping discharge, but the wave conditions determine how overtopping occurs. Larger waves give larger overtopping volumes, but less overtopping waves. From that point of view the overtopping discharge does not describe the full story of wave overtopping.

The objective of tests with the Wave Overtopping Simulator is to test the erosional strength of the crest and landward slope against wave overtopping. But do different wave conditions indeed give different moments for damage or failure of the grass? Tests performed in February and March 2010 at the Vechtdijk near Zwolle were performed with different wave conditions, in order to establish the influence of wave climate on erosional resistance. The tests have been described by Steendam et al. (2010). The wave conditions are given in Table 3.1 and can be characterized by wave heights of 1 m, 2 m and 3 m. A wave height of 1 m gives almost two times more incident waves in 6 hours than a wave height of 3 m.

| **Table 3.1 Wave conditions simulated at the Vechtdijk, Zwolle** | | | |
|---|---|---|---|
| *Seaward slope 1:4* | ***Wave height $H_s$*** | | |
| *Test duration 6 hours* | **1 m** | **2 m** | **3 m** |
| ***Peak period $T_p$ (s)*** | 4.0 | 5.7 | 6.9 |
| ***Mean period $T_m$ (s)*** | 3.3 | 4.7 | 5.8 |
| ***Number of waves $N_w$*** | 6545 | 4596 | 3724 |
| ***Run-up, $Ru_{2\%}$ (m)*** | 1.99 | 3.98 | 5.94 |

| **Table 3.2. Wave overtopping for three wave heights** | | *Mean overtopping discharge q (l/s per m)* | | | | | |
|---|---|---|---|---|---|---|---|
| | | *0.1* | *1* | *5* | *10* | *30* | *50* |
| **$H_s$ = 1 m** | *Crest freeboard $R_c$ (m)* | 2.24 | 1.63 | 1.2 | 1.02 | 0.73 | 0.6 |
| | *Percentage overtopping waves $P_{ov}$* | 0.7 | 7.2 | 24 | 35.7 | 59 | 70 |
| | *Number overtopping waves $N_{ow}$* | 45 | 471 | 1573 | 2336 | 3861 | 4583 |
| | *Maximum overtopping volume $V_{max}$ (l/m)* | 256 | 440 | 831 | 1197 | 2359 | 3401 |
| **$H_s$ = 2 m** | *Crest freeboard $R_c$ (m)* | 5.06 | 3.84 | 2.98 | 2.61 | 2.03 | 1.76 |
| | *Percentage overtopping waves $P_{ov}$* | 0.2 | 2.7 | 11.4 | 18.9 | 36.6 | 47 |
| | *Number overtopping waves $N_{ow}$* | 9 | 126 | 525 | 867 | 1683 | 2160 |
| | *Maximum overtopping volume $V_{max}$ (l/m)* | 769 | 1222 | 2018 | 2697 | 4707 | 6387 |
| **$H_s$ = 3 m** | *Crest freeboard $R_c$ (m)* | 7.98 | 6.16 | 4.89 | 4.35 | 3.48 | 3.08 |
| | *Percentage overtopping waves $P_{ov}$* | 0.085 | 1.49 | 7.05 | 12.3 | 26.1 | 34.9 |
| | *Number overtopping waves $N_{ow}$* | 3 | 55 | 262 | 456 | 972 | 1300 |
| | *Maximum overtopping volume $V_{max}$ (l/m)* | 1424 | 2254 | 3478 | 4509 | 7375 | 9709 |

The three wave conditions give different overtopping parameters, like the crest freeboard, percentage of overtopping waves, number of overtopping waves and largest overtopping wave volume, all related to a certain overtopping discharge. All these values have been given in Table 3.2. A wave height of 1 m, for example, gives for an overtopping discharge of 10 l/s per m 2336 overtopping waves in 6 hours. For a 3 m wave height this reduces to 456 overtopping waves, which is only 20% of the number for 1 m waves, but the overtopping discharge is the same. It is clear that the larger wave height will then give larger overtopping volumes, which in this example is 4.5 $m^3$/m as largest volume for a 3 m wave height and only 1.2 $m^3$/m for a 1 m wave height.

The Vechtdijk was a 100% sandy dike, covered with only 0.15 m of soil and grass. It was expected that failure of the grass would certainly be achieved for each of the wave conditions and probably for different overtopping discharges. This was, however, not always the case due to early failure of a tree in the slope and a particular transition (see Steendam 2010) and it was not always possible to reach failure of the grassed slope itself.

It became also clear that it is not so easy to decide when a grassed slope has start of damage, developing damage or failure. Failure is the most easy definition: the sand core underneath the soil layer becomes free and damage develops fast. Start of damage would actually be the first small hole in the grass cover and this is not a consistent parameter as it may depend on the existence or non-existence of one weak spot on a fairly large surface. A more consistent definition would be "various damaged locations", meaning that it does not depend solely on one weak spot. In the case the grassed slope did not fail the condition "no failure" became also a criterion.

In summary the following damage criteria were used:

- First damage (Figure 3.1)
- Various damaged locations (Figure 3.2)
- Failure (Figure 3.3)
- Non-failure after testing (Figure 3.4)

Figure 3.1. First damage.

Figure 3.2. Various damaged locations

Figure 3.3. Failure.

Figure 3.4. Non-failure after testing

The theory of shear stress with a threshold was taken as a basis for development, see also Hoffmans et al. (2008). The development, however, took place at the same time when Dean et al. (2010) worked on their erosional equivalence, but it had not yet been published at that time. Dean et al. (2010) considered three possible developments, which in essence can be described as follows:

Erosion due to excess velocity: $E = K \Sigma((u - u_c)\, t)$ [m/s] (3.1)

Erosion due to excess shear stress: $E = K \Sigma((u^2 - u^2_c)\, t)$ [$m^2$/s] (3.2)

Erosion due to excess of work: $E = K \Sigma((u^3 - u^3_c)\, t)$ [$m^3$/s] (3.3)

In all cases the velocity of the overtopping wave plays a role and a critical velocity, which should be exceeded before erosion will take place. In the equations also the time that the critical velocity is exceeded, is important.

The analysis of the Vechtdijk results had as basis Equation 3.2 (Hoffmans et al. 2008). The testing showed indeed that only waves of a certain volume (or velocity) damaged the slope. Smaller volumes did not contribute to the development of damage. This confirms the use of a threshold like $u_c$. But one main modification was made, based on observed behaviour during testing. In Equations 3.1-3.3 the time that

$u_c$ is exceeded is taken into account. The origin of this comes from tests with continuous overflow, where indeed time, or the duration that the flow is present, is important.

But (severe) wave overtopping is different from continuous overflow. First of all, velocities in an overtopping wave are much larger than velocities in continuous overflow, for the same discharge. Secondly, the duration that $u_c$ is exceeded in an overtopping wave is quite short, in the order of 1-3 s, and this duration is fairly constant and in total much shorter than for continuous overflow.

The observation of overtopping waves has taught us that a wave front rushes over the slope with large velocity. Within tenths of seconds the maximum velocity is reached. The grass feels this as a kind of "impact" and it is this impact that causes initiation or further development of damage. It is believed that this impact is more important than the duration of the overtopping wave above a certain threshold. For this reason Equation 3.2 was rewritten to an erosional index called "cumulative overload", where the actual time or duration for an overtopping wave was omitted:

$$\text{Cumulative overload: } \Sigma(u^2 - u_c^2) \quad [m^2/s^2] \qquad (3.4)$$

With known distributions of overtopping wave volumes and known velocities per overtopping wave volume it is possible to calculate the cumulative overload for each wave overtopping condition, or a number of tests, to a certain moment when a damage criterion is reached. And the cumulative overload depends of course on the critical velocity $u_c$ that is taken.

The main question is then: what is the critical velocity, $u_c$, that brings the damage observed for different hydraulic regimes, together?

The four damage criteria (see Figures 3.1-3.4) were taken for all tests and the results were compared for critical velocities of 0; 3.1; 4.0; 5.0 and 6.3 m/s, which are in accordance with overtopping wave volumes of 0; 0.25; 0.5; 1 and 2 $m^3/m$. Figures 3.5-3.7 give the comparison for the extremes (0 and 6.3 m/s) and for 4.0 m/s.

The transition and the tree for a wave height of 2 m failed before the grass failed and the test had to be stopped before grass failure could be reached. These are the columns for "non-failure". The grass did fail, however, for the tests with 1 m and 3 m wave height, each after a different test duration. The section for 1 m wave height failed after 6 hours tests with 0.1; 1; 10; 30 l/s per m and another 2:07 hours with 50 l/s per m. The section with 3 m wave height failed after 6 hours tests with 0.1; 1; 10 l/s per m and another 1:03 hour with 30 l/s per m. The large wave height gave earlier damage and for both wave heights the damage was mainly caused by many mole holes just below the crest.

Figures 3.5-3.7 can be used to establish the correct critical velocity for this dike section. If the height of the columns in the graphs are equal, then the correct critical velocity is found. As "non-failure" is only found for one wave height of 2 m and "first damage" is not very reliable, the most interesting columns are those for "various damages" and for "failure". Both Figures 3.5 and 3.7 show that the columns have different height. The best graph is given in Figure 3.6, where the critical velocity used was 4 m/s. This is the critical velocity that should be used for this sandy dike.

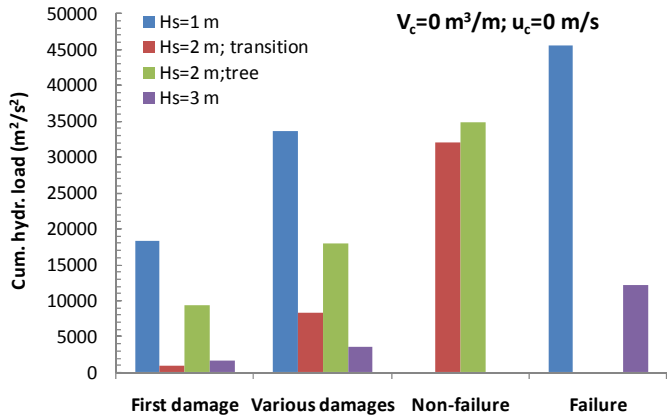


Figure 3.5. Comparison of cumulative overload for various damage criteria; $u_c$ = 0 m/s.

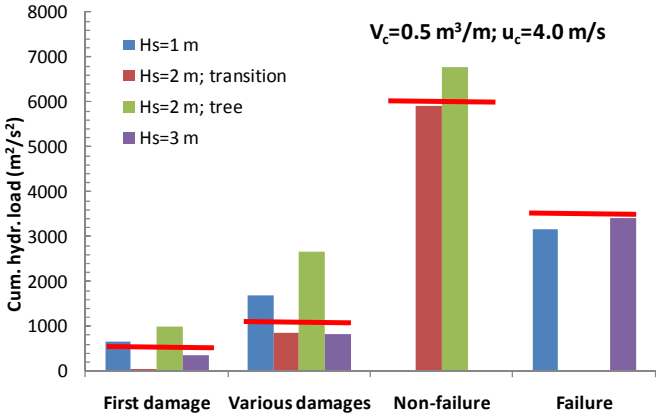


Figure 3.6. Comparison of cumulative overload for various damage criteria; $u_c$ = 4 m/s.

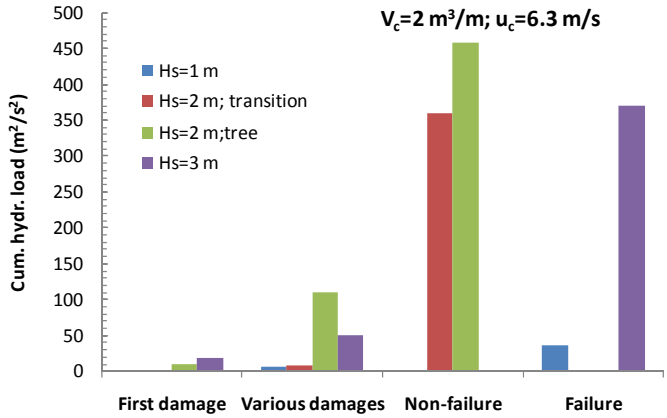


Figure 3.7. Comparison of cumulative overload for various damage criteria; $u_c$ = 6.3 m/s.

Based on Figure 3.6 the following conclusions can be made for the Vechtdijk and the limits are given in the graph:

*A critical velocity should be used of $u_c$ = 4 m/s ($V_c$ = 0.5 m³/m)*

- Start of damage: $\Sigma(u^2 - u_c^2) = 500$ m²/s²
- Various damaged locations: $\Sigma(u^2 - u_c^2) = 1000$ m²/s²
- Failure (by mole holes): $\Sigma(u^2 - u_c^2) = 3500$ m²/s²
- Non-failure for normal slope: $\Sigma(u^2 - u_c^2) < 6000$ m²/s²

A confirmation of above analysis and conclusions could be established by looking at the damage on the slope after the hydraulic measurements at the Vechtdike. Here only about 40 overtopping waves rushed down the slope instead of many hours like for normal testing, but many large volumes were present. The hypothesis of cumulative overload should work for many hours of testing, but also for the "artificial" distribution of a small number, but mainly very large overtopping waves.

The observation of the slope after the hydraulic measurements could best be described as "various damaged locations". A number of small holes were observed and one location with a little larger damaged area. The cumulative overload for these 40 waves, using $u_c$ = 4 m/s, amounted to 946 $m^2/s^2$. This is very well comparable with the 1000 $m^2/s^2$ that was given for this damage criterion. It can be concluded that this very short session of large waves can very well be compared with many hours of testing of real wave overtopping. The analysis confirmed the hypothesis of cumulative overload. But of course, more validation is required.

In future also the method of "excess of work" (Equation 3.3), which was preferred by Dean et al. (2010), should be elaborated, maybe with ongoing work in the US with a new Wave Overtopping Simulator. The reason for Dean et al., however, to choose for excess of work instead of excess of shear stress was that excess of work fitted better to known stability curves for continuous overflow, not wave overtopping. Dean et al. (2010) did not possess the results of simulation of wave overtopping at real dikes as in the Netherlands.

Another difference between the two methods is the value of the critical velocity $u_c$. Based on continuous overflow critical velocities are in the range of 1-2 m/s. But the very "weak" Vechtdijk (sand with a very thin layer of soil with grass) needs a critical velocity of 4 m/s and this can be considered as a lower boundary. Other dike sections tested need probably a critical velocity in the range of 5-7 m/s. It is, therefore, still an open question which method would work best with real wave overtopping at dikes.

After development of the prediction method with the results of the Vechtdike (overtopping for different wave heights), all earlier results were analyzed again in order to get an idea about the critical velocity, which actually gives the strength of the grass cover, for the dike slopes tested. The first conclusion was that *failure* of a grassed slope by wave overtopping occurs for 3500 $m^2/s^2$. Failure means large hole(s) in the slope with fast increase of damage. The analysis resulted in the following estimated critical velocities for the dike slopes tested, with between brackets the overtopping wave volume that produces that velocity.

| | |
|---|---|
| Delfzijl: | 6.3 m/s (2 $m^3$/m) - assumption that slope could resist more than 50 l/s per m |
| Boonweg: | 6.3 m/s (2 $m^3$/m) |
| St Philipsland: | 5 m/s (1 $m^3$/m) |
| Kattendijke: | 6.3 m/s (2 $m^3$/m) |
| Afsluitdijk: | > 6.3 m/s (> 2 $m^3$/m) |
| Vechtdijk: | 4 m/s (0,5 $m^3$/m) |

The description of the grass cover of each tested location is given in the mentioned reports. It includes a description of the species of grass, root coverage, clay/sand properties, etc. Together with the estimated critical velocities it should be a basis to develop a method to predict the critical velocity (strength) of a given slope. This method still has to be developed further.

The method of cumulative overload has been developed into an easy to apply format. The full method is not given here, but only an example. The first parameter to assess is the critical velocity or strength of the slope, based on results described above. Then

the cumulative overload can be calculated as follows. From theory we can calculate the overtopping discharge for any wave condition. The overtopping discharge gives also the distribution of overtopping wave volumes and each volume has a specific velocity. The cumulative overload can then be calculated for a fixed period of wave overtopping, for various critical velocities and various wave conditions. The easy to apply method consists then of a graph for a specific critical velocity.

Figure 3.8 gives the method for a critical *velocity of 5 m/s*. The graph was made for a wave overtopping *duration of 1 hour*. The graph shows the cumulative overload as a function of the overtopping discharge and different curves have been given for different wave heights. The wave heights cover the range of $H_s$ = 0.5 - 4 m. It is assumed that the wave steepness is $s_{op}$ = 0.04.

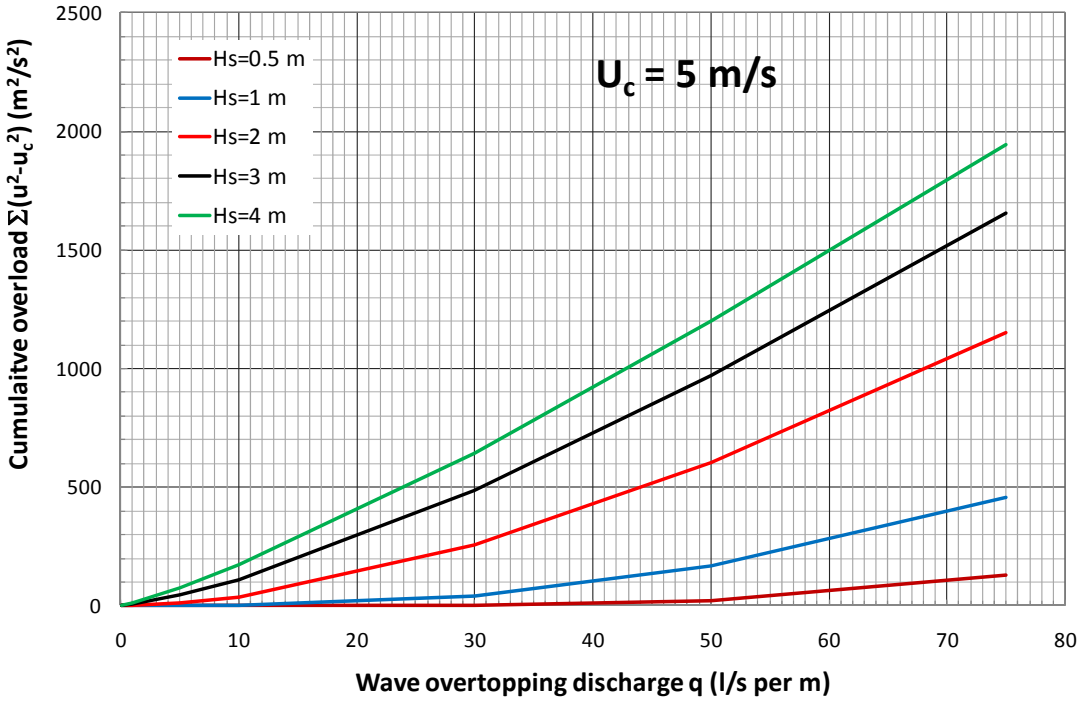


Figure 3.8. Prediction method, showing the cumulative overload as a function of overtopping discharge and wave conditions. Overtopping duration is 1 hour; $u_c$ = 5 m/s.

One can enter the graph with the wave height and overtopping discharge for a specific case. This gives, often through interpolation, the cumulative overload for 1 hour of overtopping. This value should then be recalculated for the actual duration of overtopping. It is also possible to calculate a sequence of overtopping conditions (simulating the tide or development of storm surge) and establish the cumulative overload for each sequence. The total cumulative overload is simply the summation of all individual cumulative overloads.

## 3.3 Prediction method for the Wave Run-up Simulator

The wave action in the run-up and run-down zone is different from that at the crest and landward slope by wave overtopping. At the seaward side water flows two ways (up and down the slope) and the velocity on the slope is not directly correlated with a wave volume.

Nevertheless, if velocities in the run-up and run-down zone would be known, for the entire zone, the method of cumulative overload can directly be applied. It is for this reason that the next part of this report has been focused on theoretical description of

these velocities in the run-up and rundown zone. The outcome can be applied to the prediction method, but is also the boundary condition to develop the Wave Run-up Simulator as the new Simulator has to produce the correct velocities, as well as run-up levels.

This means also that possible testing with the Wave Run-up Simulator can rely on all the results from the wave overtopping tests and that testing is mainly to validate the prediction method.

# 4 Run-up velocities and flow depths from direct measurements

## 4.1 General

Some researchers have looked at various zones of the wave-structure interaction at a dike, as given in Figure 1.4. Those researchers with work from the previous century are mentioned in the PhD-thesis of Schüttrumpf (2001). Schüttrumpf performed small scale and large scale tests on wave run-up and wave overtopping and measured and analyzed amongst others velocities and flow depths. His work is a main basis. At the same period Van Gent (2002) performed flume tests on wave overtopping and also measured velocities and flow depths at crest and landward slope. A combined paper was given by Schüttrumpf and Van Gent (2003), summarizing the two investigations.

Bosman (2008) tried to explain the differences between the results as described in Schüttrumpf and Van Gent (2003), by introducing a slope angle into the equations. Later work under the EU Hydralab project Flowdike did not validate Bosman's hypothesis and the final conclusion might be that there is quite some uncertainty or scatter in predicting wave run-up velocities or flow depths. This chapter will summarize all the work mentioned.

A simple way to look at wave run-down velocities is to consider kinetic and potential energy and leave any influence of friction out of the equations (Van der Meer and Klein Breteler, 1990):

$$E_{kin} = E_{pot} \qquad (4.1)$$

$E_{kin} = 0.5\ m\ u_d^2$ and $E_{pot} = mg(R_u - z_A)$, with:

$E_{kin}$ = kinetic energy
$E_{pot}$ = potential energy
$m$ = mass of water particle
$u_d$ = run-down velocity
$g$ = acceleration of gravity
$R_u$ = maximum level of wave run-up related to the still water level swl
$z_A$ = location on the seaward slope, in the run-down zone, related to swl

Elaboration gives:

$$u_d = (2g(R_u - z_A)^{0.5} \qquad (4.2)$$

The velocity is simply related to the vertical difference with the run-up level. A similar equation would be valid for the run-up velocity and in general terms one could formulate the run-up velocity as:

$$u = c_u\ (g(R_u - z_A)^{0.5} \qquad (4.3)$$

The coefficient $c_u$ has to be established by research. With no friction and the assumption that run-up would be similar to run-down velocity, a first estimation of $c_u$ is $2^{0.5}$ or roughly 1.4. But there is always some friction, giving a little larger value, and the process of run-up is not exactly equal to run-down. Often the 2%-value is taken for $u_{2\%}$, as well as for $Ru_{2\%}$. This may also give some differences, but a value around $c_u = 1.4$ has to be expected.

Schüttrumpf (2001) gives also the theoretical elaboration including a friction term. Eq. 4.3 is used by Van Gent (2002), but Schüttrumpf uses the following equation:

$$u/(\pi H_s/T_m) = a_0 \cot\alpha\ \xi\ (g(R_u - z_A)^{0.5} \quad (4.4)$$

where:
$H_s$ = significant wave height at the to of the structure
$T_m$ = mean wave period
$a_0$ = coefficient
$\alpha$ = slope angle
$\xi$ = surf similarity parameter of breaker parameter, $\xi = \tan\alpha/(2\pi H_s/(gT_m^2))$

Using the definition of $\xi$, however, modifies Equation 4.4 to:

$$u = (\pi/2)^{0.5}\ a_0\ (g(R_u - z_A)^{0.5} \quad (4.5)$$

This gives $u_c = (\pi/2)^{0.5}\ a_0$ and all values of Schüttrumpf of $a_0$ can directly be rewritten to $u_c$.

There is no theoretical assumption for the flow depth, h, during run-up. Assuming a linear decrease for flow depth from swl to the run-up level gives the following relationship:

$$h = c_h\ (R_u - z_A) \quad (4.6)$$

By only considering random waves and the 2% values, the equations for run-up velocity and flow depth become:

$$u_{2\%} = c_{u2\%}\ (g(R_u - z_A)^{0.5} \quad (4.7)$$

$$h_{2\%} = c_{h2\%}\ (R_{u2\%} - z_A) \quad (4.8)$$

## 4.2 Flow depth

Van Gent (2002) produced waves on a 1:100 sloping foreshore with deep and shallow conditions and with uni-modal and bi-modal waves. His structure had a slope of 1:4. At the transition from upper slope to crest he found, see also Figure 4.1, $c_{h2\%} = 0.15$.

He validated his equations with two other independent investigations. The tests in Delft Hydraulics' report H24 (seaward slope about 1:4) gave $c_{h2\%} = 0.21$ (Figure 4.2) and in a similar report H1256 (seaward slopes of 1:3, 1:4 and 1:4 with a berm) again gave $c_{h2\%} = 0.21$ (Figure 4.3). Both values are larger than in Van Gent's own work.

Schüttrumpf (2001) describes two investigations, a small scale investigation on slopes of 1:4 and 1:6 (described in LWI Bericht 852) and a large scale investigation on a slope of 1:6 (LWI Bericht 858). Two types of spectra were used in the large scale investigation, a TMA spectrum and natural (measured) sea spectra. In his original work the coefficients for flow depth are given depending on slope angle, but rewritten he found the following coefficients for the flow depth:

| | |
|---|---|
| Small scale, slope 1:4 | $c_{h2\%} = 0.22$, see Figure 4.4 |
| Small scale, slope 1:6 | $c_{h2\%} = 0.21$, see Figure 4.4 |
| Large scale, slope 1:6 | $c_{h2\%} = 0.33$ (TMA spectra), see Figure 4.5 |
| Large scale, slope 1:6 | $c_{h2\%} = 0.34$ (Natural spectra), see Figure 4.6 |

The small scale investigation shows similar coefficients as for H24 and H1256, but the large scale investigation gives 50% larger coefficients and more than double of Van Gent (2002).

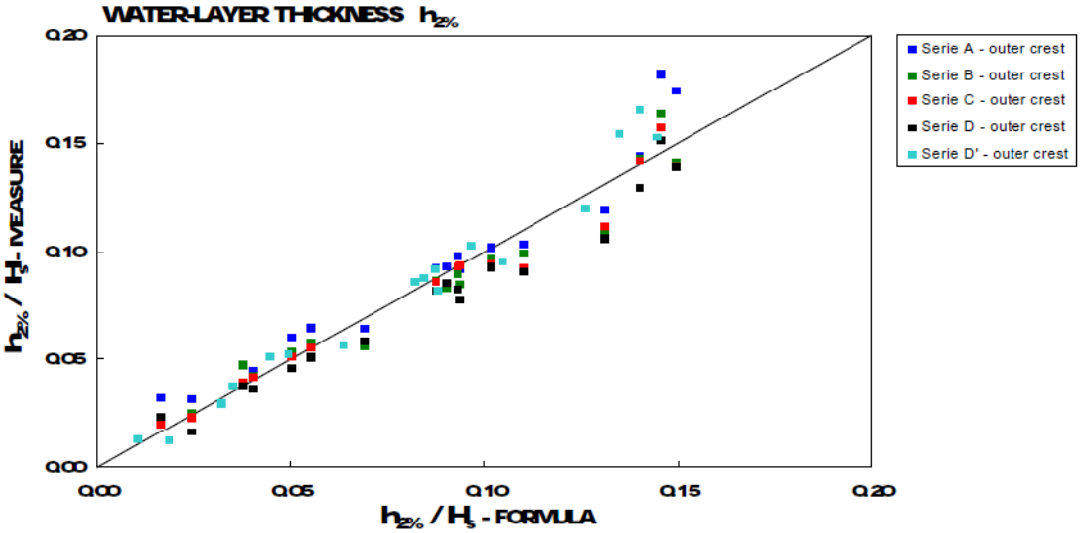


Figure 3.2 Water-layer thickness at seaward side of the crest (Series A-D'); data compared to Equation 3.2.

Figure 4.1. Measurements by Van Gent (2002) (taken from Van Gent (2002).

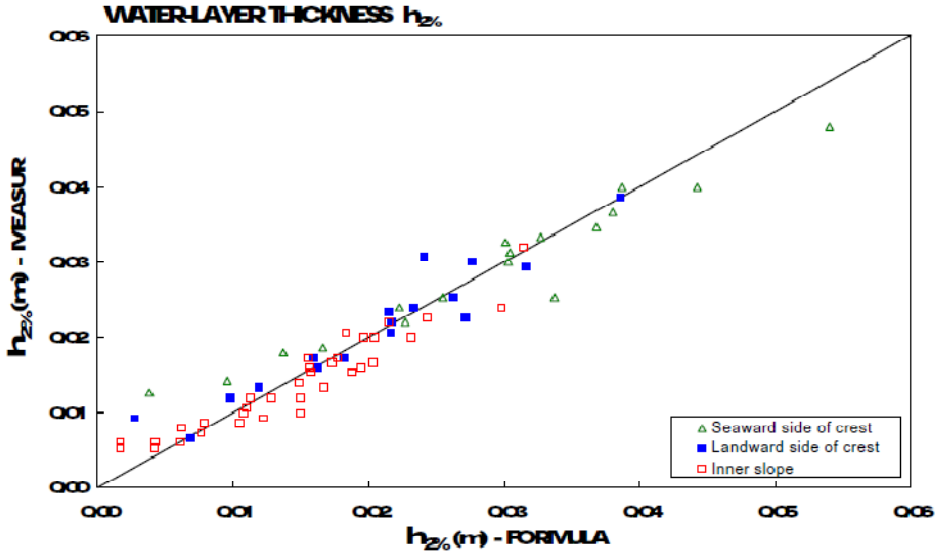


Figure 3.23 Water-layer thickness at crest and inner slope (H24).

Figure 4.2. Flow depth in H24 (taken from Van Gent, 2002).

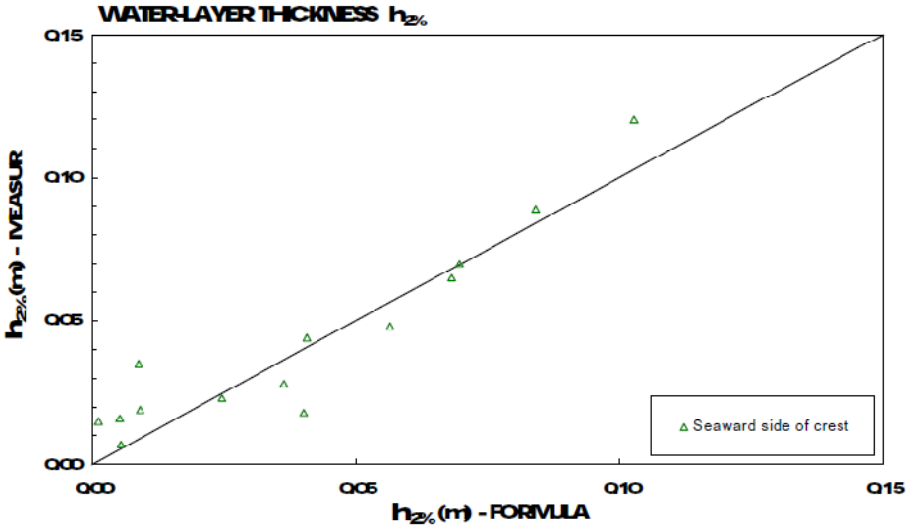


Figure 3.26 Water-layer thickness at seaward side of crest (H1256).

Figure 4.3. Flow depth in H1256 (taken from Van Gent, 2002).

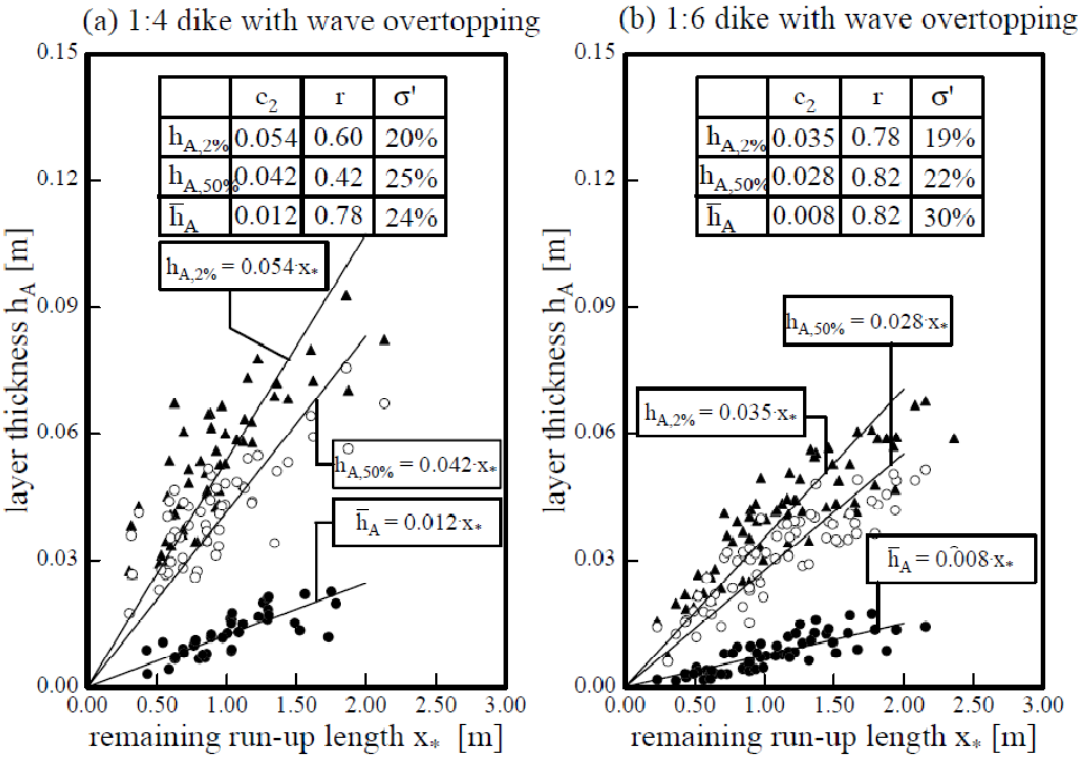


| | $c_2$ | r | σ' |
|---|---|---|---|
| $h_{A,2\%}$ | 0.054 | 0.60 | 20% |
| $h_{A,50\%}$ | 0.042 | 0.42 | 25% |
| $\bar{h}_A$ | 0.012 | 0.78 | 24% |

| | $c_2$ | r | σ' |
|---|---|---|---|
| $h_{A,2\%}$ | 0.035 | 0.78 | 19% |
| $h_{A,50\%}$ | 0.028 | 0.82 | 22% |
| $\bar{h}_A$ | 0.008 | 0.82 | 30% |

**Fig 8:** Layer thickness of wave run-up as a function of the remaining wave run-up length $x_*$

Figure 4.4. Small scale tests of Schüttrumpf (2001). Values of c2 should be multiplied by cotα in order to get ch2%. Figure from Schüttrumpf and Oumeraci (2005), similar to Figure 4.13b in Schüttrumpf (2001).

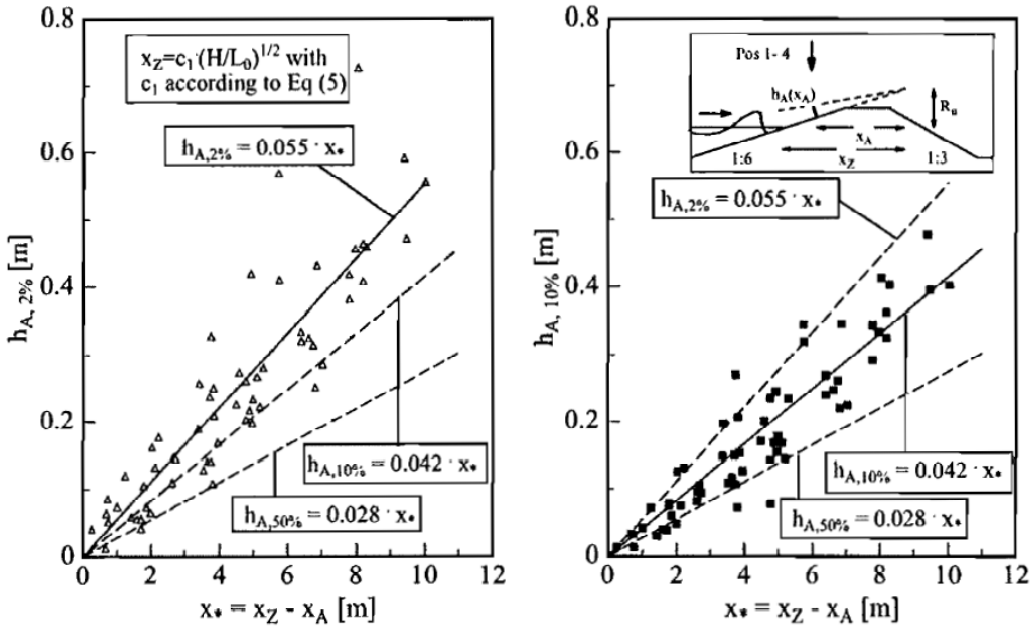


Fig. 44: Layer Thickness on the seaward slope for TMA spectra: $h_{A,2\%}$ (left) and $h_{A,10\%}$ (right)

Figure 4.5. Large scale tests on 1:6 slope for TMA spectra. Coefficient in hA2% should be multiplied by 6 to get ch2%. From LWI Bericht 858.

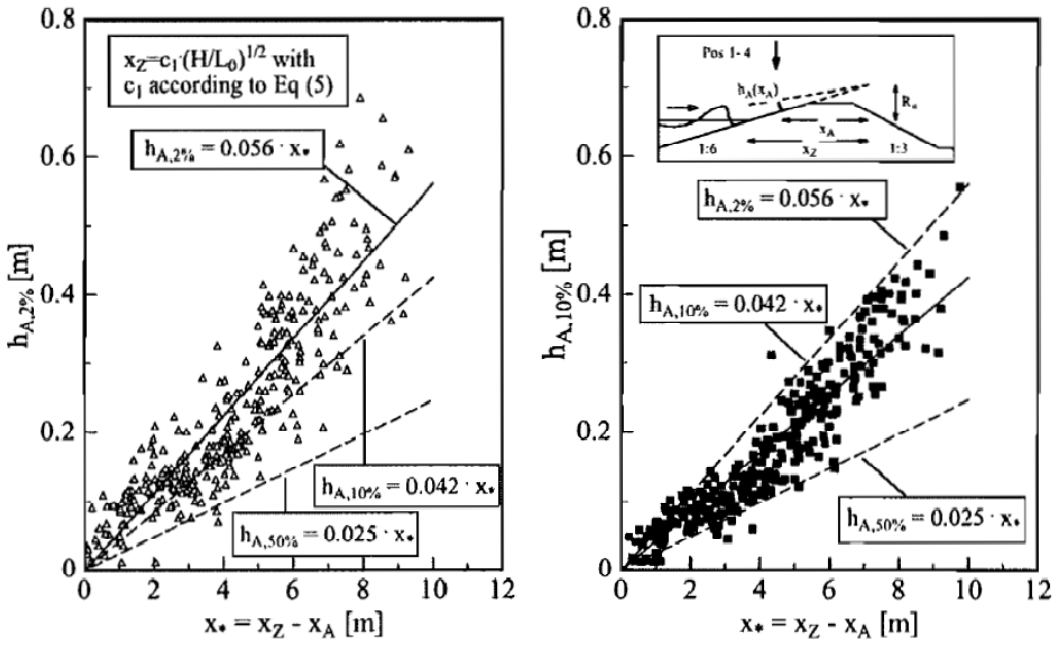


Fig. 46: Layer Thickness on the seaward slope for natural wave spectra (see Figures 15 and 16): $h_{A,2\%}$ (left) and $h_{A,10\%}$ (right)

Figure 4.6. Large scale tests on 1:6 slope for Natural spectra. Coefficient in hA2% should be multiplied by 6 to get ch2%. From LWI Bericht 858.

In Schüttrumpf et al. (2002) $c_{h2\%}$ = 0.33 is given, based on the large scale tests with TMA spectra. The reason for this choice is not given.

In Schüttrumpf and Van Gent (2003) the value $c_{h2\%}$ = 0.33 is given for Schüttrumpf's work and the value $c_{h2\%}$ = 0.15 for Van Gent's work. The difference is more than a factor of 2.

The EurOtop Manual (2007) gives $c_{h2\%}$ = 0.055 cotα, but reference is made to "TMA" spectra, suggesting that reference was the 1:6 large scale testing, giving $c_{h2\%}$ = 0.33 for a 1:6 slope, but also $c_{h2\%}$ = 0.22 for a 1:4 slope. This latter value is closer to the other values.

Bosman (2008) worked on an explanation of the difference between Van Gent's and Schüttrumpf's flow depth coefficients. Looking at the small and large scale tests of Schüttrumpf (2001), the difference is also in these tests: $c_{h2\%}$ = 0.22 for a 1:6 small scale test and $c_{h2\%}$ = 0.33 for a 1:6 large scale test. From this point of view it is not the slope angle that caused the difference. An explanation for Schüttrumpf's choice for $c_{h2\%}$ = 0.33 (large scale testing) in later papers and the EurOtop Manaul (2007) may-be that the small scale tests were only performed for 100 s. This means that the 2% value is the largest wave in the series and not very reliable. But even then the difference between values of 0.22 and 0.33 is large.

Bosman (2008) only reanalyzed five tests of the large scale data of Schüttrumpf (2001). He came to the conclusion that the slope angle should be involved:

$$h_{2\%} = 0.010/\sin^2\alpha \, (R_{u2\%} - z_A) \qquad (4.9)$$

This would give $c_{h2\%}$ = 0.17 for a 1:4 slope and 0.37 for a 1:6 slope. As sinα and cotα are almost similar for small slope angles, Equation 4.9 can also be written as:

$$h_{2\%} = 0.010 \cot^2\alpha \, (R_{u2\%} - z_A) \qquad (4.10)$$

Figure 4.7 gives the data without the influence of slope angle and indeed gives a large difference. Figure 4.8 is according to Equation 4.10 and shows a good correlation. But actually all existing data should be considered to come to a validation.

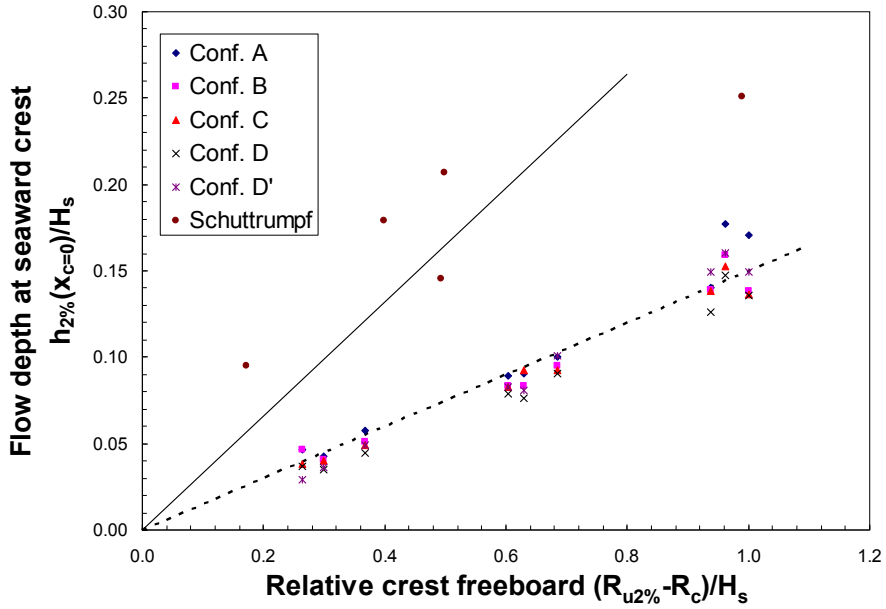


Figure 4.7. Flow depth at the seaward crest by Schüttrumpf (2001) and Van Gent (2002) as given by Bosman (2008). Only five tests of Schüttrumpf were used.

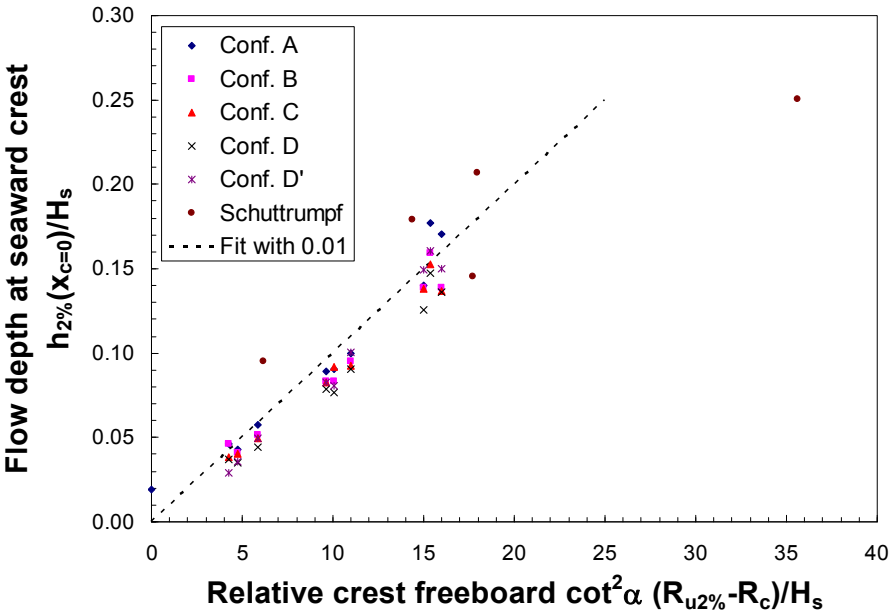


Figure 4.8. Flow depth at the seaward crest by Schüttrumpf (2001) and Van Gent (2002) as given by Bosman (2008), including the slope angle as in Equation 4.10. Only five tests of Schüttrumpf were used.

Recently tests were performed under the EU Hydralab project Flowdike. First results have been described by Lorke et al. (2010). The main objective was to investigate the influence of current on wave overtopping, including oblique waves. But reference tests were performed with perpendicular wave attack and without current. Velocities at the crest were measured by micro-propellers and flow depths by thin wave gauges. Flowdike 1 tested a 1:3 slope (start of 2009), where later Flowdike 2 looked at a 1:6 slope (end of 2009). First analysis of Flowdike 1 gave the results presented in Figure 4.8.

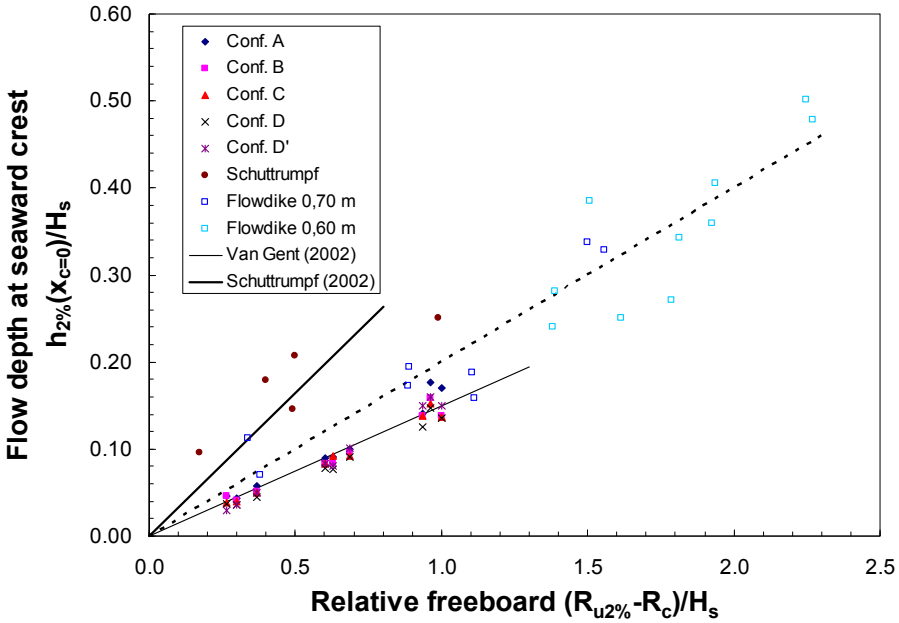


Figure 4.9. Flow depth at the seaward crest, including Flowdike 1 data.

The data of the 1:3 slope are in between the 1:6 and 1:4 slope, which does not validate Bosman's theory with Equation 10. According to Flowdike 1 $c_{h2\%}$= 0.20, very close to many of the other data groups described.

In Flowdike 2 a wave gauge was located on the seaward slope, about 0.12 m from the crest, which on a 1:6 slope is 0.02 m below the crest. Also a wave gauge was located 0.03 m beyond the crest. Figure 4.10 gives the data, added to the data present in Figure 4.9. Flow depths for the 1:6 data of Flowdike 2 are larger than for the 1:3 data of Flowdike 1 and are actually quite close to the 5 data points of Schüttrumpf. A fit through the Flowdike 2 data would give $c_{h2\%}$= 0.29.

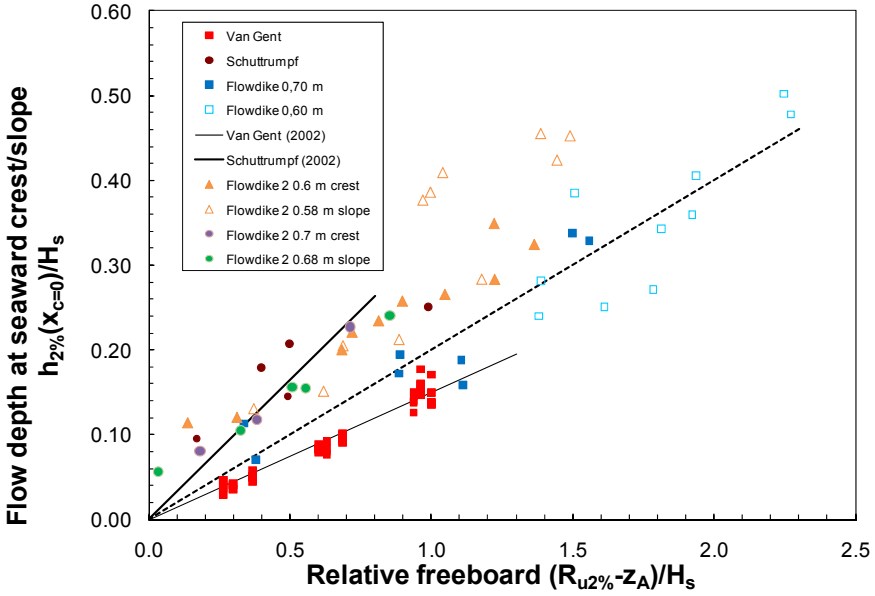


Figure 4.10. Flow depth at the seaward crest and slope, including Flowdike 1 (1:3) and Flowdike 2 (1:6) data.

## 4.3 Run-up velocities

A similar analysis as performed in Section 4.2 on flow depth can be done for run-up velocities.

Van Gent (2002) found for his 1:4 slope $c_{u2\%}$= 1.3 at the seaward crest, see Figure 4.11 for his results. His tests with a smooth crest showed an *increase* in velocity along the crest and at the landward slope he found $c_{u2\%}$= 1.7. This is opposite to other investigations where flow velocity along the crest normally slows down a little. On the other hand, most of the data in Figure 4.11 are above the line, except for Series D, which means that the coefficient of $c_{u2\%}$= 1.3 in reality could be a little larger.

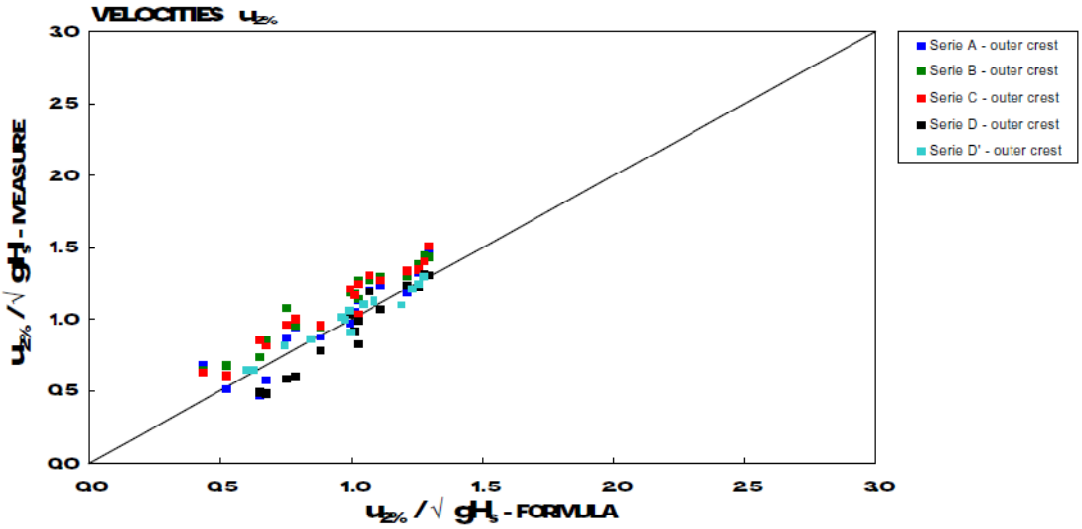


Figure 3.3 Velocities at seaward side of the crest (Series A-D'); data compared to Equation 3.3.

Figure 4.11. Measurements by Van Gent (2002) (taken from Van Gent (2002).

He validated his equations with one other independent investigation. The tests in Delft Hydraulics' report H24 (seaward slope about 1:4) gave $c_{u2\%}$ = 1.7 (Figure 4.12). In this case it were front velocities measured over the narrow crest by looking at the time difference between two gauges. The value is similar to Van Gent's value for the landward side of the crest. Note in Figure 4.12 that only 3 values for the crest are above the line, all others are lower. This indicates that a better coefficient would be a little smaller than 1.7.

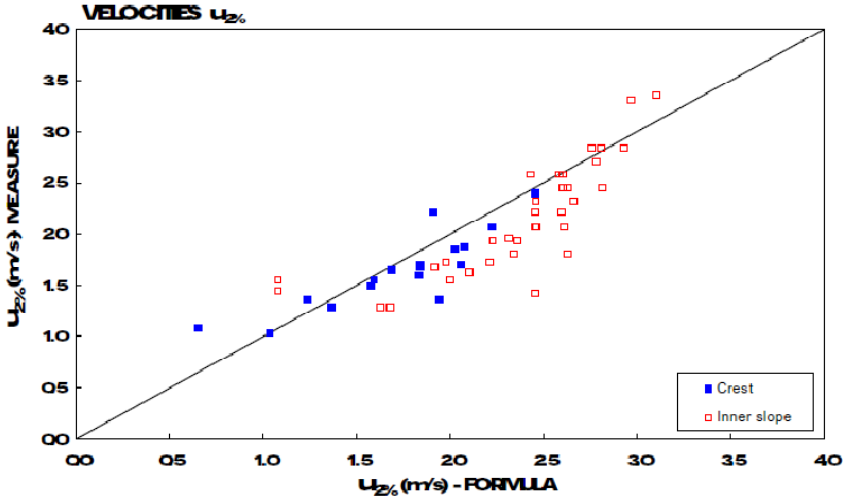


Figure 3.24 Velocities at crest and inner slope (H24).

Figure 4.12. Flow velocity at crest in H24 (taken from Van Gent, 2002).

As noted before, Schüttrumpf (2001) describes two investigations, a small scale investigation on slopes of 1:4 and 1:6 (described in LWI Bericht 852) and a large scale investigation on a slope of 1:6 (LWI Bericht 858). Two types of spectra were used in the large scale investigation, a TMA spectrum and natural (measured) sea spectra.

The small scale investigation gave $u_{50\%}$, not the 2% values. This may be due to the very short test duration of 100 s. The large scale tests gave the following results:

Large scale, slope 1:6 $c_{u2\%}$ = 1.55 (TMA spectra), see Table 4.1
Large scale, slope 1:6 $c_{u2\%}$ = 1.39 (Natural spectra), see Fig. 4.13 and Table 4.1.

The original values of $a_0$ = 1.11 and 1.24 were recalculated with $u_c = (\pi/2)^{0.5}\, a_0$, see also Equation 4.5. The values of 1.55 and 1.39 are between the two values of 1.3 and 1.7, given by Van Gent (2002).

| | | $a_0^*$ | r | σ | |
|---|---|---|---|---|---|
| regular waves | $v_A$ | 1.03 | r=0.93 | σ=3.80 | large scale model tests |
| | | 0.75 | r=0.92 | - | small scale model tests (SCHÜTTRUMPF, 2001) |
| TMA spectra | $v_{A,50\%}$ | 0.82 | r=0.78 | σ=2.27 | large scale model tests |
| | | 0.75 | r=0.91 | - | small scale model tests (SCHÜTTRUMPF, 2001) |
| | $v_{A,10\%}$ | 1.09 | r=0.86 | σ= 2.26 | large scale model tests |
| | $v_{A,2\%}$ | 1.24 | r=0.89 | σ= 2.52 | large scale model tests |
| natural wave spectra | $v_{A,50\%}$ | 0.76 | r=0.98 | σ=1.06 | large scale model tests |
| | $v_{A,10\%}$ | 0.98 | r=0.90 | σ= 1.75 | large scale model tests |
| | $v_{A,2\%}$ | 1.11 | r=0.90 | σ=2.26 | large scale model tests |

Table 4.1. Large scale results for TMA and natural spectra (from LWI Bericht 858).

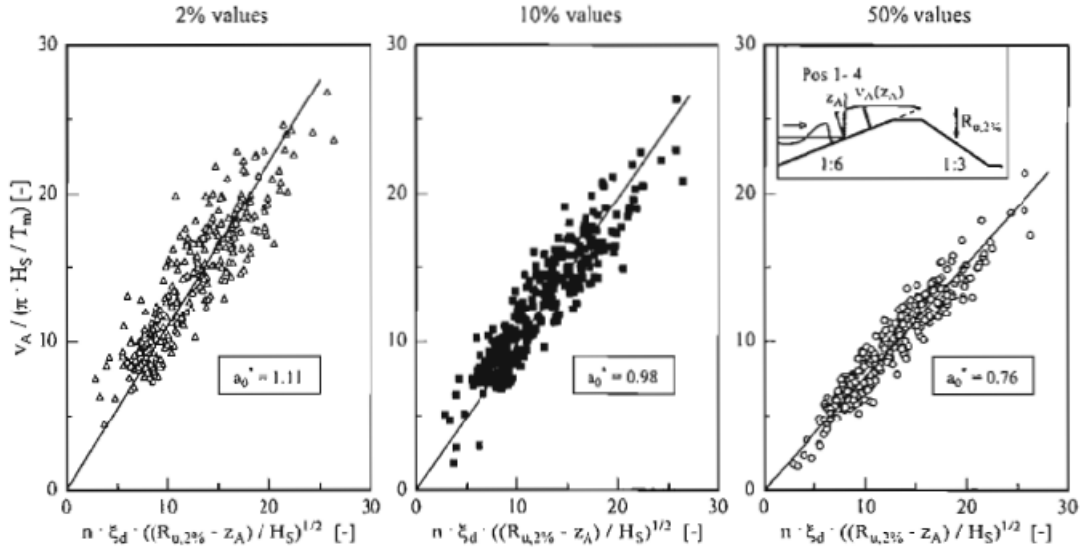


Fig. 49: Wave run-up velocity on the seaward slope for natural wave spectra

Figure 4.13. Large scale results on velocity for natural spectra (from LWI Bericht 858).

In Schüttrumpf and Van Gent (2003) $c_{u2\%}$ = 1.37 is given for Schüttrumpf's work and $c_{u2\%}$ = 1.3 for Van Gent. It is not clear where this 1.37 comes from as it is different from the values 1.39 and 1.55 mentioned earlier.

The Wave Overtopping Simulator has been designed for $c_{u2\%}$ = 1.35, in between the two values given in Schüttrumpf and Van Gent (2003).

EurOtop (2007), however, gives $c_{u2\%}$ = 1.55, which is the value from the large scale tests with TMA spectra.

Bosman (2008) included the slope and if sinα is replaced by cotα, then $c_{u2\%}$ = 0.30 cotα. Flowdike 1 (see Lorke et al., 2010 for an overall view) validated more or less this assumption. Figure 4.14 shows the data of Van Gent (2002), the five data points used by Bosman of Schüttrumpf (2001) and the data of Flowdike 1. The 1:6 data are on the left side of the graph, the 1:3 Flowdike data are on the right side and the 1:4 data of Van Gent (2002) are in the middle. Figure 4.15 shows the same Figure, but now with a cotα included. The data are now grouped together. The best fit gave $c_{u2\%}$ = 0.35 cotα.

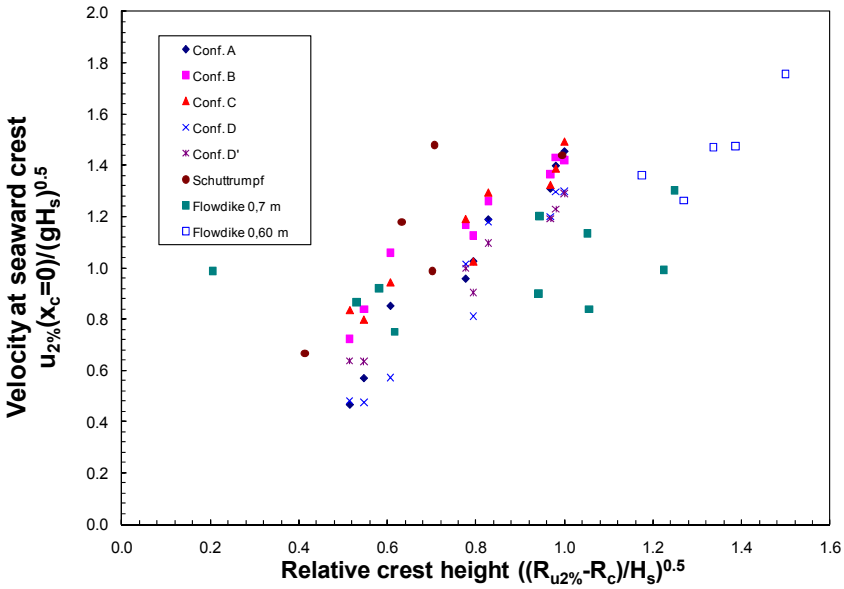


Figure 4.14. Results of Schüttrumpf (1:6), Van Gent (1:4) and Flowdike 1 (1:3)

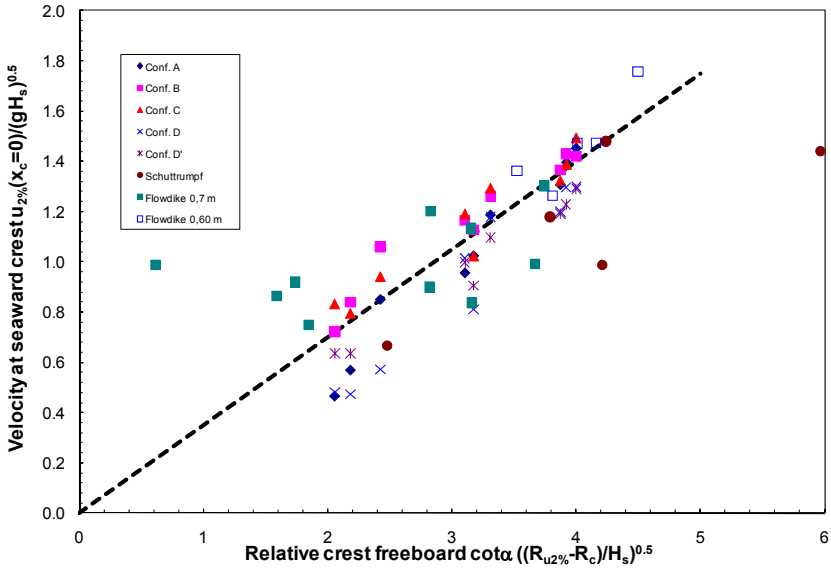


Figure 4.15. Results of Schüttrumpf (1:6), Van Gent (1:4) and Flowdike 1 (1:3), including cotα.

Velocities were also measured in Flowdike 2 for a slope of 1:6. Data has not yet been analyzed in depth. The measurements show a large difference between velocity at the seaward crest and the landward crest, which cannot be correct. Figure 4.16 gives the results with the data of Figure 4.14 as comparison. The data are all on the right side of the graph, where the other 1:6 data are on the left side. For the time being, Flowdike 2 data are considered not to be reliable.

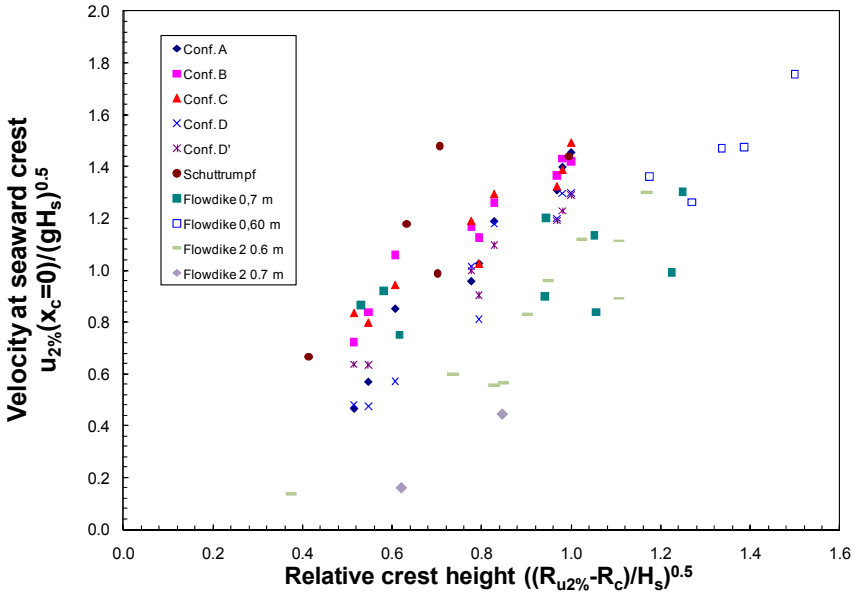


Figure 4.16. Data from Figure 18 with Flowdike 2 data on a 1:6 slope added.

## 4.4 Discussion on results

Table 4.2 shows a summary of results for $c_{h2\%}$ and $c_{u2\%}$, more or less in chronicle order.

It seems that both values by Van Gent's work are on the lower side, although his data has minor scatter and the fit with his data is quite good. Four independent other sources give for slopes around 1:3 and 1:4 a value of $c_{h2\%}$ = 0.20-0.22. The large scale 1:6 tests, but also the 1:6 Flowdike 2 tests give a value $c_{h2\%}$ = 0.29-0.34. Only the small scale 1:6 slope gives the lower value of $c_{h2\%}$ = 0.21, but these tests are probably less accurate as the test duration was only 100 s.

| **Authors** | **Seaward slope, cotα** | **$c_{h2\%}$** | **$c_{u2\%}$** |
|---|---|---|---|
| Van Gent (2002) | 4 | 0.15 | 1.3 |
| Van Gent H24 (2002) | 4 | 0.21 | 1.7 |
| Van Gent H1256 (2002) | 3; 4; 4+berm | 0.21 | |
| Schüttrumpf (2001) small scale | 4 | 0.22 | |
| Schüttrumpf (2001) small scale | 6 | 0.21 | |
| Schüttrumpf (2001) large scale TMA | 6 | 0.33 | 1.55 |
| Schüttrumpf (2001) large scale | 6 | 0.34 | 1.39 |
| Schüttrumpf et al. (2002) | 6 | 0.33 | 1.55 |
| Schüttrumpf and Van Gent (2003) | 4; 6 | 0.33/0.15 | 1.37/1.3 |
| EurOtop (2007) | - | 0.055cotα | 1.55 |
| Bosman (2008) | 4; 6 | $0.10\cot^2\alpha$ | 0.30cotα |
| Flowdike 1 - Lorke et al. (2010) | 3 | 0.20 | 0.35cotα |
| Flowdike 2 - Lorke et al. (2010) | 6 | 0.29 | |

Table 4.2. Summary of results on velocity and flow depth coefficients on the seaward slope or seaward crest.

There seems to be a difference between the gentle slope of 1:6 and the steeper slopes of 1:3 and 1:4, but there is no real difference between these steeper slopes of 1:3 and 1:4. This makes it difficult to give a relationship with cotα.

**A conclusion could be to take $c_{h2\%}$ = 0.20 for slopes of 1:3 and 1:4 and $c_{h2\%}$ = 0.30 for a slope of 1:6. Consequently, a slope of 1:5 would then by interpolation give $c_{h2\%}$ = 0.25. This procedure is better than to use a formula like $c_{h2\%}$ = 0.055 cotα, as given in EurOtop (2007).**

From theory (Section 4.1) one might expect that $c_{u2\%}$ should be equal or larger than 1.4. Only Van Gent (2002) shows a little smaller value, but it was noted in Section 4.4 that based on his data one may except a little larger value than 1.3. In the same section it was argued that the high value of 1.7 for the H24 data could be a little lower.

Schüttrumpf's large scale data give $c_{u2\%}$ values of 1.39 and 1.55. This is well in between the values of Van Gent. In EurOtop (2007) the larger value was chosen. The Flowdike 1 analysis gave $c_{u2\%}$ = 0.35 cotα, leading to values of 1.05; 1.4 and 2.1 for slopes of 1:3; 1:4 and 1:6. Specially the value for the 1:6 slope is too large.

**A conclusion could be to take $c_{u2\%}$ = 1.4-1.5 for slopes between 1:3 and 1:6.**

But the main conclusion is that all research that is compared in the present analysis is not always consistent. This may be due to the fact that measurement of velocities and flow depths on structures is not easy, certainly not at a large scale where turbulence and air entrainment may affect the measurements. Or that assumptions, like a linear decrease, are not correct. Moreover, many measurements were performed at the transition between slope and crest, where the wave changes from up-rushing to horizontal. This could also give some extra scatter.

## 4.5 Other probabilities than 2%

In Sections 4.2-4.5 only the 2% value has been evaluated. Schüttrumpf (2001) has mentioned other exceedance percentages like 10% and 50%. The H24 data set gave graphs of exceedance curves of velocities and flow depths at the crest and landward slope of a (small scale) dike. The curves were plotted on a Rayleigh scale, which means that a Rayleigh distribution is shown as a straight line in such a graph. Figures 4.17 and 4.18 give an example of measured flow depths (Figure 4.17) and velocities (Figure 4.18). The general conclusion was that flow depth and velocity are indeed Rayleigh distributed.

This conclusion can be used to calculate other exceedance probabilities. A similar procedure is used to calculate the percentage of overtopping waves. Based on the assumption that the run-up distribution is Rayleigh distributed, the overtopping percentage or number of overtopping waves can be calculated for any other crest height.

The equation is:

$$P_x = \exp\left[ - \{(-\ln(0.02))^{0.5}\, c_{x\%}/c_{2\%}\}^2\right] \qquad (4.11)$$

where $P_x$ = probability and $c_{x\%}$ = the coefficient to be used to calculate the flow depth or velocity with Equations 4.7 and 4.8.

The ratio $c_{x\%}/c_{2\%}$ becomes 0.77 for $P_x$ = 10% and 0.42 for $P_x$ = 50%.

Figure 4.5 gives gives $c_{h2\%}$ = 0.55; $c_{h10\%}$ = 0.042 and $c_{h50\%}$ = 0.028. With the two given ratio's the values, according to a Rayleigh distribution would be $c_{h10\%}$ = 0.042 and $c_{h50\%}$ = 0.023. Figure 4.6 gives $c_{h2\%}$ = 0.56; $c_{h10\%}$ = 0.042 and $c_{50\%}$ = 0.025. According

to a Rayleigh distribution this becomes $c_{h10\%}$ = 0.042 and $c_{50\%}$ = 0.023. Prediction and measurements are very close for the flow depth coefficient $c_h$.

Table 4.1 gives values for the velocity coefficient $c_u$. For the TMA spectra $c_{u2\%}$ = 1.24; $c_{u10\%}$ = 1.09 and $c_{u50\%}$ = 0.82. With the two given ratio's the values, according to a Rayleigh distribution would be $c_{u10\%}$ = 0.84 and $c_{u50\%}$ = 0.52. For the natural spectra $c_{u2\%}$ = 1.11; $c_{u10\%}$ = 0.98 and $c_{u50\%}$ = 0.0.76 is found. With a Rayleigh distribution this would become $c_{u10\%}$ = 0.85 and $c_{u50\%}$ = 0.47. The calculated values are much smaller than the measured ones, which suggests that in these cases the distribution of velocities is not according to Rayleigh.

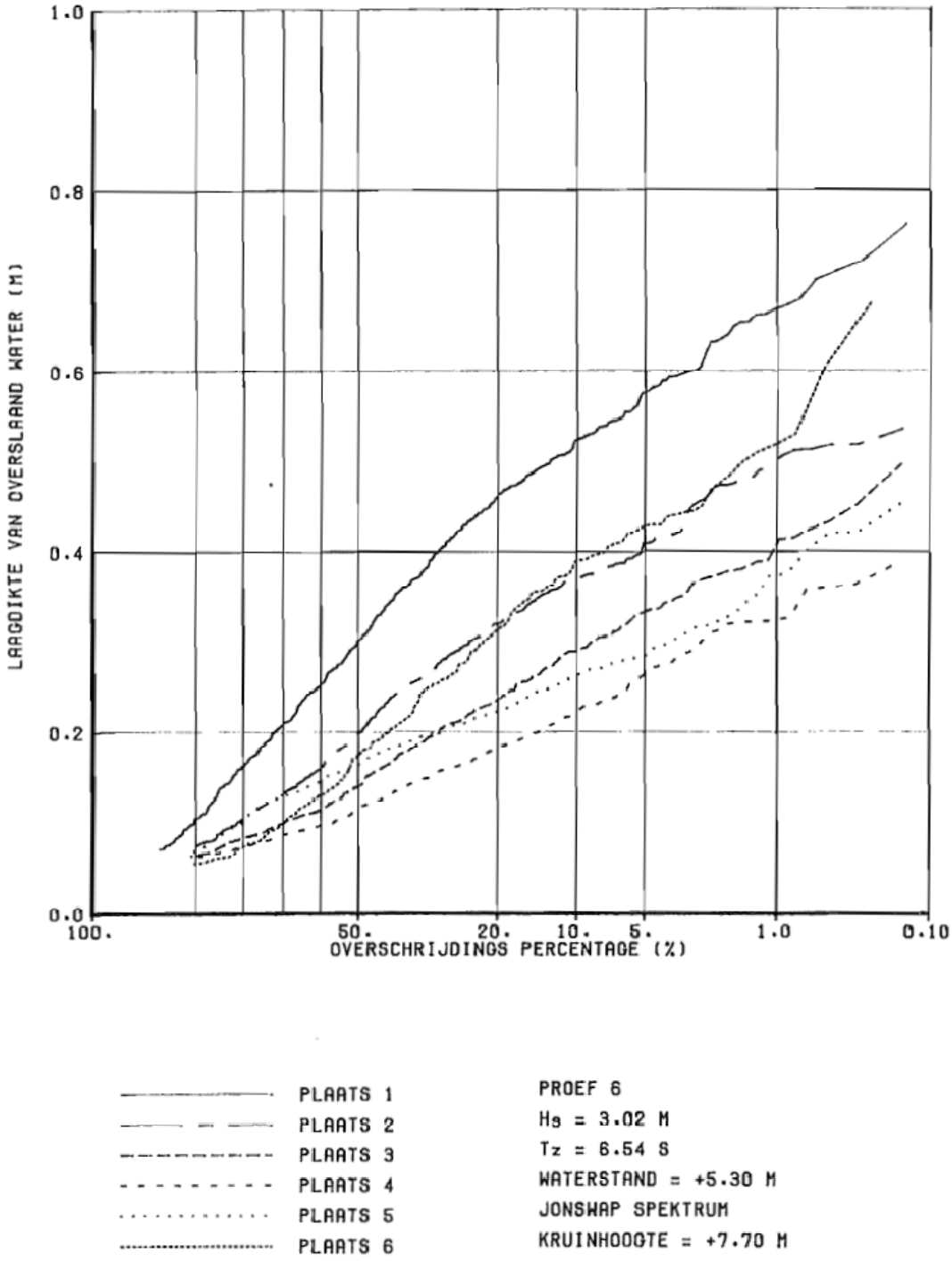


Figure 4.17. Flow depths at the crest and landward slope of a small scale dike. Data from H24.

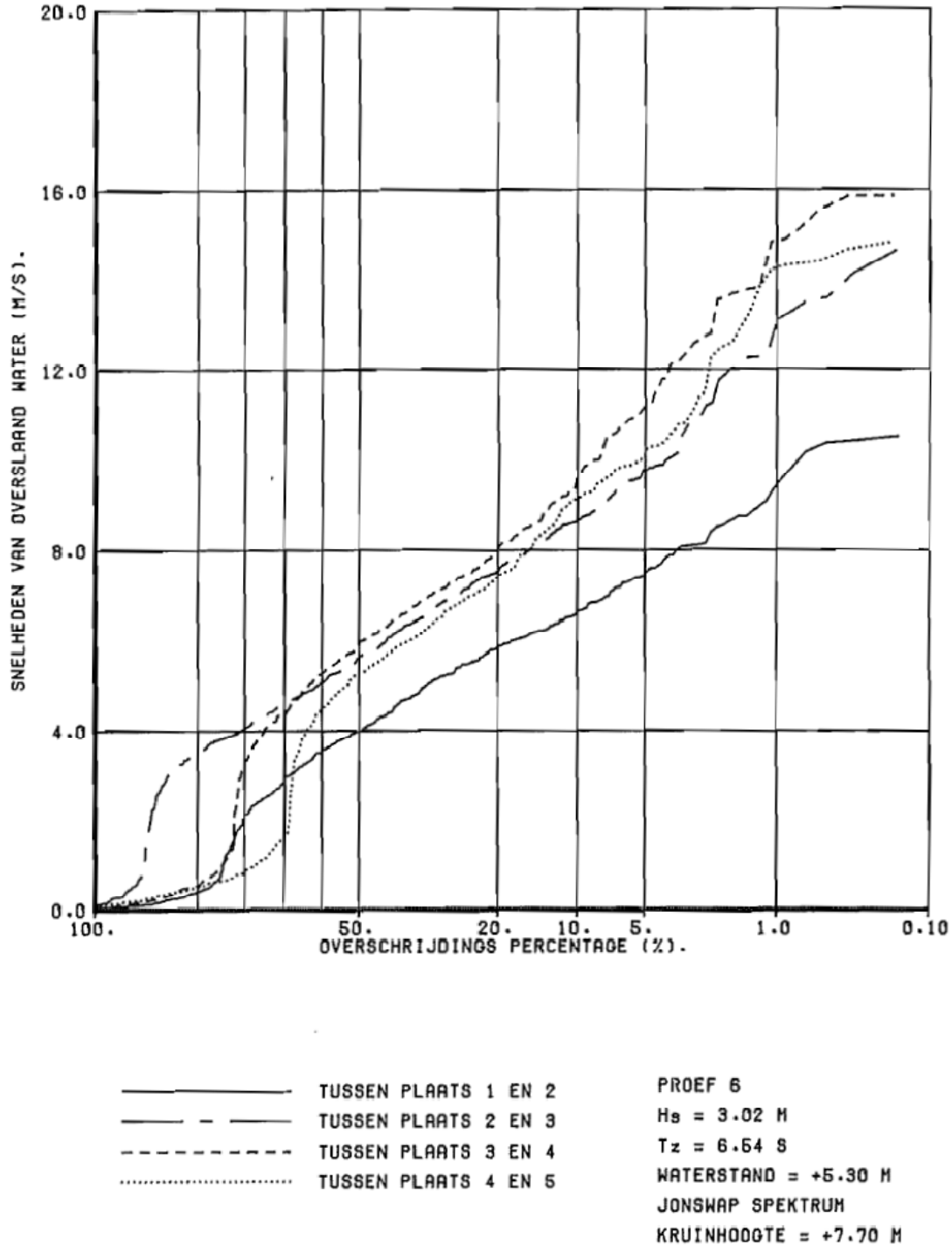


Figure 4.18. Velocities at the crest and landward slope of a small scale dike (front velocities). Data from H24.

# 5 Velocities based on analysis of run-up gauge records

## 5.1 Introduction

The analysis in Chapter 4 was mainly based on direct measurement of velocity and flow depth and often at the crest of an overtopped structure and at the landward slope. Direct measurement of velocities has been performed with propellers or electromagnetic velocity meters, sometimes by calculation of front velocities between wave gauges. Analysis was focused on the 2% exceedance value at the crest.

There is not much research which has focused on run-up and run-down velocities along the seaward slope. But there is research that measured wave run-up along a non-overtopping slope. The records of these type of measurements show the location of the up-rushing wave front along the slope. The derivative of the change of location gives a front velocity, in the same way as the front velocity can be calculated between two fixed points. The advantage of the wave run-up record is that it shows the front velocity over the full run-up zone. This type of records will be analysed in this chapter. The run-up gauge does not show flow depths and, therefore, the analysis is limited to flow velocity only.

Three data sets were available with the raw data of a wave run-up gauge:

- Flowdike I on a slope 1:3;
- Flowdike II on a slope 1:6;
- Petten seadike; real measurements on the 1:3 upper slope of a seadike.

The Flowdike I and II measurements have a similar set-up, but a different slope. The two slopes of 1:3 and 1:6 cover a large range of slopes applied in reality. Figure 5.1 shows the set-up in Flowdike 1. Wave overtopping was measured on two different crest levels (with two overtopping tanks for each crest) and wave run-up was measured by a capacitance wire stretched just above a slope, which was high enough to prevent wave overtopping.

Figure 5.1. Test set-up in Flowdike I on measuring wave run-up and overtopping.

At the Petten sea dike a wave run-up gauge has been constructed by means of cells, that detect whether there is water or not. Figure 5.2 shows the run-up gauge, seen from the crest of the dike downwards. The down slope is 1:4, then a 11 m long berm of 1:20 at a level of 5 m +NAP and finally a 1:3 upper slope till a crest height of 12 m +NAP. Measurements were performed during a severe storm on 9 November 2007. The wave height close to the dike was about 2.2 m with a spectral period $T_{m-1,0}$ = 10 s and the water level was about 2.75 m. This storm condition was more or less constant during 3 hours and 40 minutes, giving 1436 incident waves.

Figure 5.2. Wave run-up gauge at the Petten Seadike, seen from the crest downwards.

The Flowdike measurements were performed with a set of six wave boundary conditions: three wave heights with for each wave height two wave steepnesses. Such a set was required to get enough data on wave overtopping. For wave run-up the crest height does not play a role and the three wave heights are actually scale tests (a two times smaller wave height should give a two times smaller wave run-up).

The two wave steepnesses were $s_{op}$ = 0.02 and 0.04, where $s_{op}$ is the deep water wave steepness, calculated with the peak period $T_p$. Storm waves without depth limitation have often a wave steepness close to 0.04. If waves break due to a shallow foreshore, like along the North Sea coast at Petten, the wave steepness reduces to 0.02 or even smaller. The range of wave steepness between 0.02 and 0.04 covers a large part of storm conditions along the Dutch coast.

From Flowdike I and II five tests were selected which cover the range of slopes 1:3 and 1:6 and wave steepnesses between 0.02 and 0.04, see Table 5.1. One test was chosen to check the validity of the "scale test".

| | | | | | |
|---|---|---|---|---|---|
| Flowdike I | slope 1:3 | test 148 | $H_s$ = 0.145 m | $T_p$ = 2.16 s | $s_{op}$ = 0.02 |
| Flowdike I | slope 1:3 | test 149 | $H_s$ = 0.145 m | $T_p$ = 1.52 s | $s_{op}$ = 0.04 |
| Flowdike I | slope 1:3 | test 146 | $H_s$ = 0.098 m | $T_p$ = 1.78 s | $s_{op}$ = 0.02 |
| Flowdike II | slope 1:6 | test 456 | $H_s$ = 0.150 m | $T_p$ = 2.13 s | $s_{op}$ = 0.02 |
| Flowdike II | slope 1:6 | test 457 | $H_s$ = 0.140 m | $T_p$ = 1.51 s | $s_{op}$ = 0.04 |

Table 5.1. Selected tests from Flowdike I and II

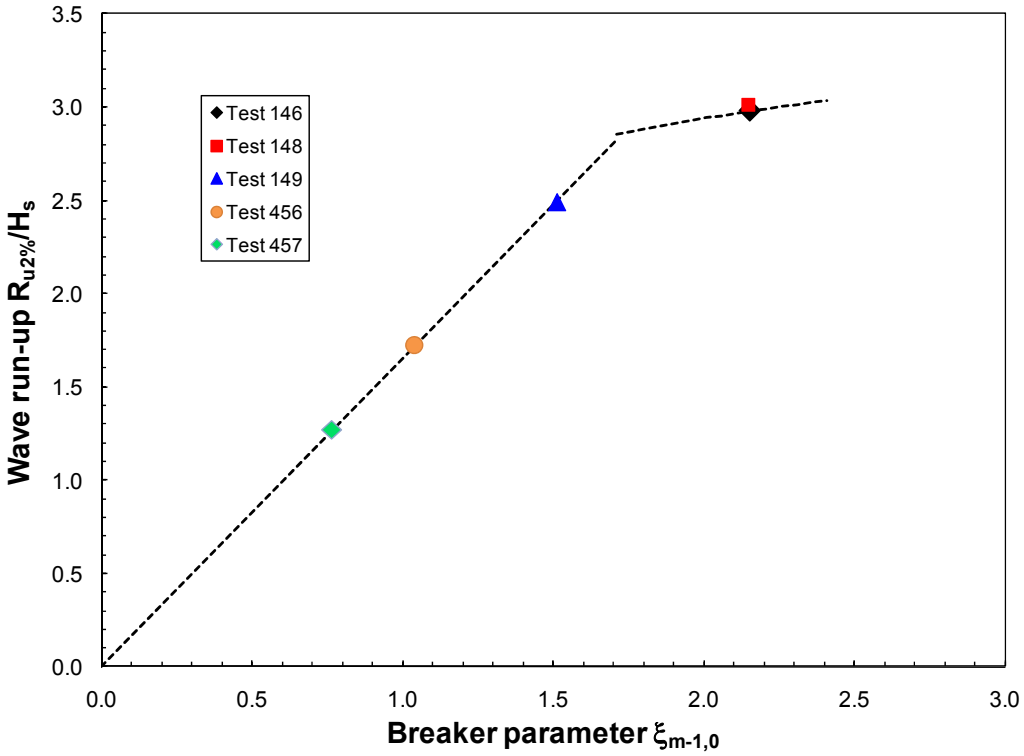


Figure 5.3. 2%-Run-up data compared with EurOtop prediction.

Figure 5.3 gives the measured 2%-run-up values of the five tests of Flowdike and are compared with the prediction of 2%-run-up from the EurOtop Manual (2007). The comparison is extremely good! The graph also shows that the five tests give a good range over the breaker parameter from $\xi_{m-1,0}$ = 0.8 - 2.2. Moreover, the "scale tests" 146 and 148 give the same dimensionless run-up. The graph shows that these five tests cover a large range in slope angles as well as wave steepnesses.

Figures 5.4 - 5.6 give examples of wave run-up measurements of three records. Test 148 of Flowdike I (Figure 5.4) shows a nice signal. The signal of test 456 (Figure 5.5) of Flowdike II has a kind of fast vibration over the main signal, which has to be removed. The wave run-up gauge at the Petten Seadike (Figure 5.6) starts at a level of 5.72 m +NAP, which is almost 3 m higher than the storm surge level. It gives only the highest part of the up-rushing waves. The up-rushing part is a nice signal.

Front velocities can be obtained from the record of the wave run-up by taking a certain distance that the front has passed over the slope in a certain time. First of all the wave run-up signal has to be smooth, otherwise the velocities will show a large variation. The signal of test 456 has been smoothed by a 4 points moving average and becomes then quite smooth, see Figure 5.8.

The sampling frequency of the measurements was different for each data set. Flowdike I used 0.04 s, Flowdike II 0.025 s and the measurements at Petten Seadike were performed with 0.1 s. Figure 5.7 shows the calculated velocity signals calculated

over 0.04 s; 0.08 s and 0.16 s. The first signals show a lot of fast variations, the last one is more steady. The front velocity calculated over 0.16 s was used for further analysis. Figure 5.8 shows calculated front velocities over 0.1 s; 0.2 s and 0.25 s. The last one with 0.25 s does not show large variations and was used for further analysis. Figure 5.9 gives the front velocity at the Petten Seadike, calculated over 0.8 s, which was considered as quite reliable.

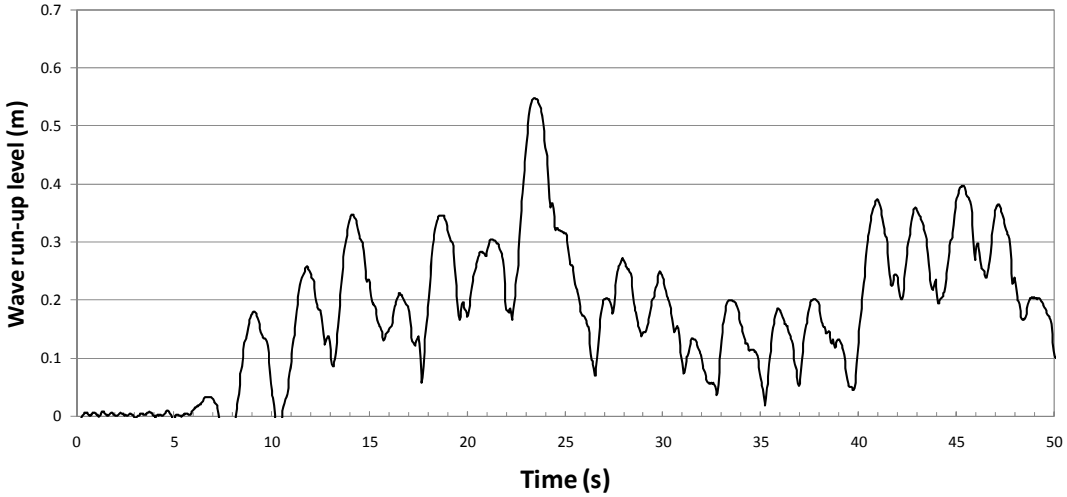


Figure 5.4. Wave run-up for the first 50 s of test 148 on slope 1:3.

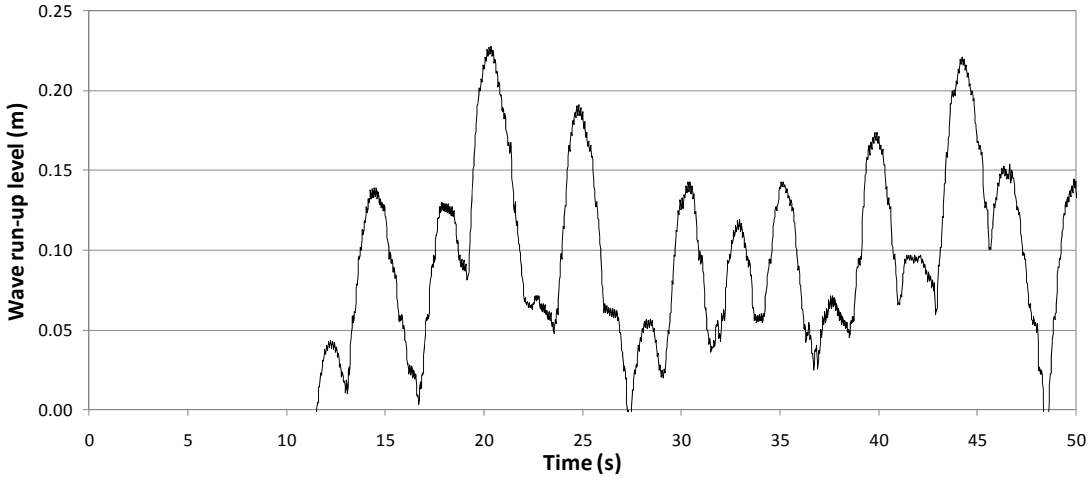


Figure 5.5. Wave run-up for the first 50 s of test 456 on slope 1:6.

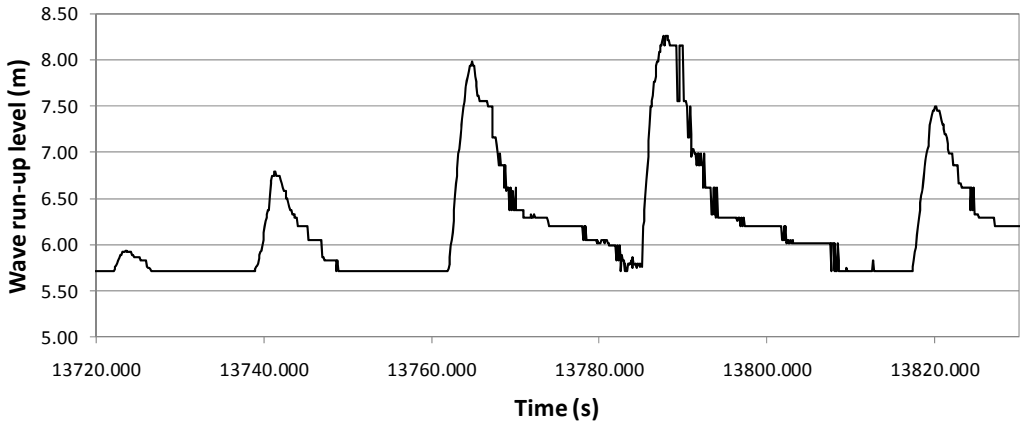


Figure 5.6. Wave run-up for almost two minutes, measurements at Petten Seadike, 9 November 2007

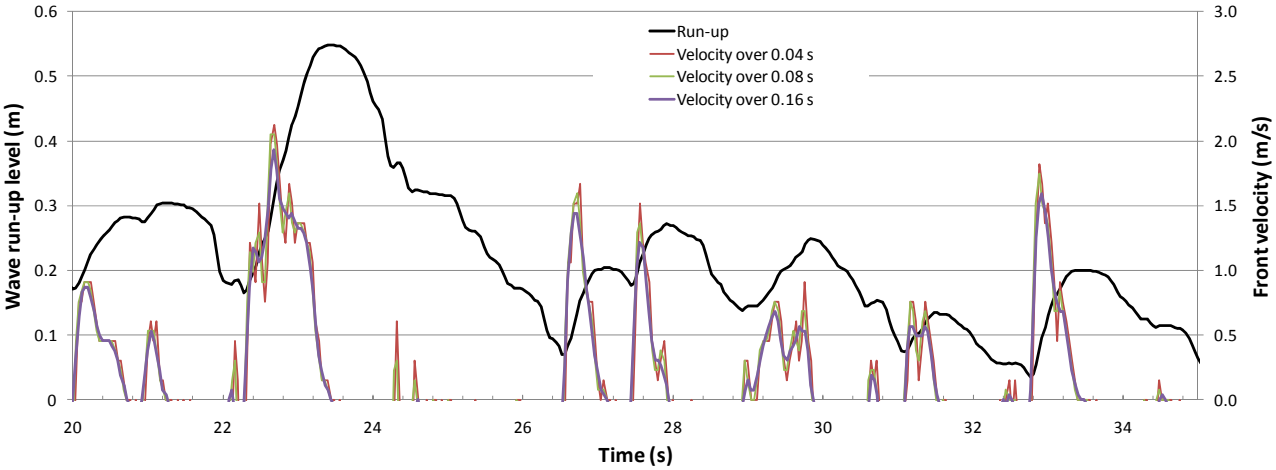


Figure 5.7. Wave run-up and front velocities for test 148; slope 1:3.

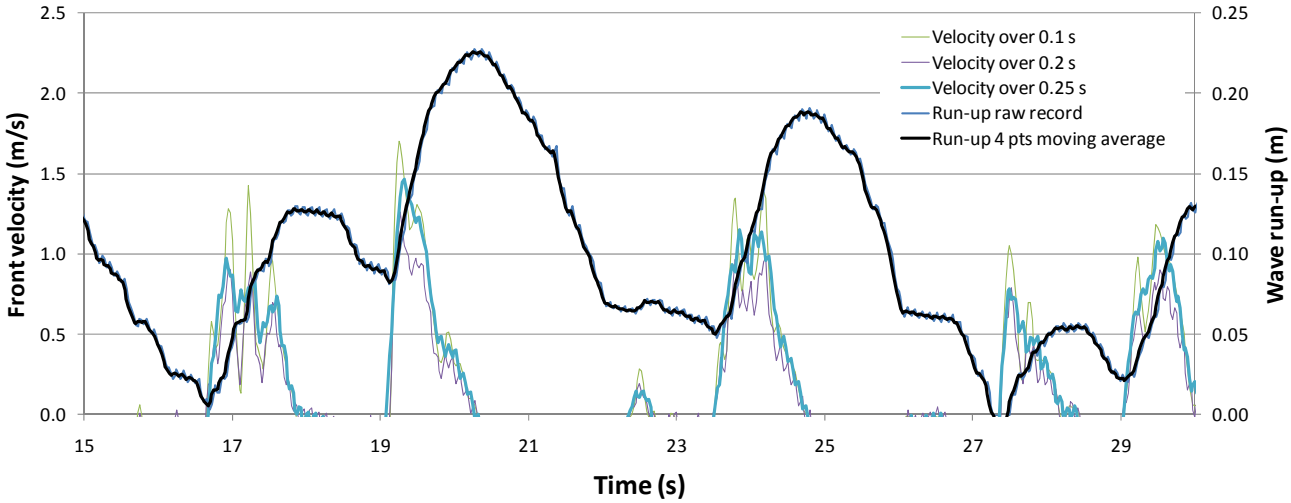


Figure 5.8. Wave run-up and front velocities for test 456; slope 1:6.

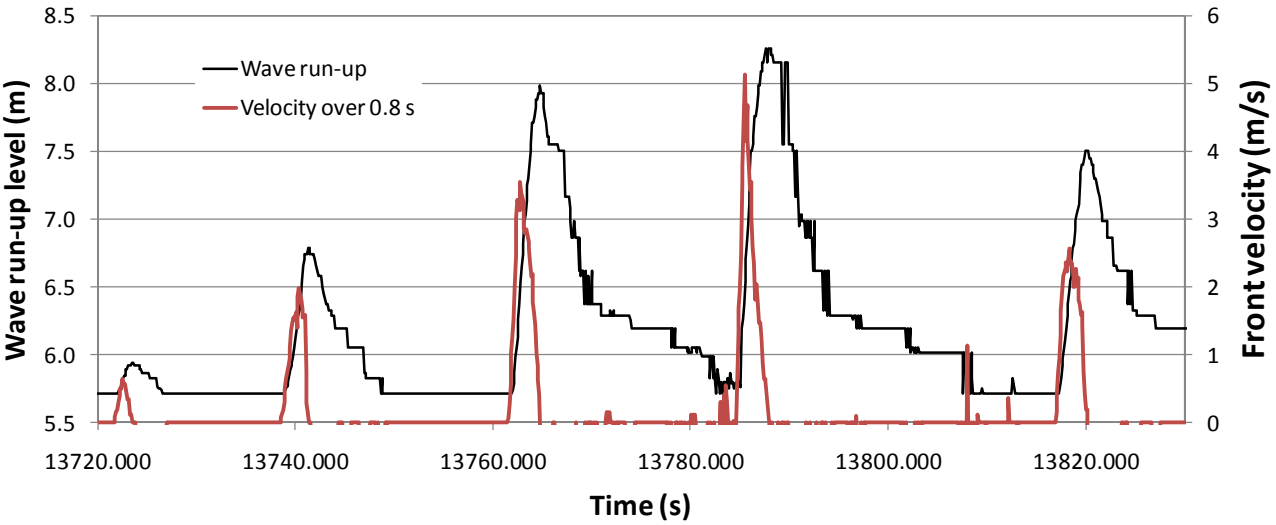


Figure 5.9. Wave run-up and front velocities at Petten Seadike

The velocity records were analyzed further, together with the wave run-up records. This analysis has been described in the next section.

## 5.2 Analysis of front velocities in the run-up zone

The prediction method for strength of grass covers at the crest and landward side of a dike (the cumulative overload method, see Chapter 3) depends on velocities exceeding a certain critical velocity. Only fairly large velocities contribute to initial or ongoing damage of the grass cover. It is for this reason that analysis of the front velocities was focused on the large velocities only, say the largest 10-20% of the velocities.

The maximum velocities were taken from this largest part. The run-up signal, however, gives also the location where this maximum velocity was found, as well as the maximum run-up level for that specific wave. The location of the maximum velocity has some variation, as it was calculated over some time. Certainly when the run-down suddenly changes into run-up, it takes some time before the maximum velocity is calculated as a maximum. The real location for the maximum velocities, therefore, may be a little lower on the slope than calculated.

Maximum velocities, the location of this velocity on the slope and the maximum wave run-up of that specific wave were found by data processing. A closer inspection of Figures 5.4-5.6 as well as Figures 5.7-5.9 shows that often the first part of the wave run-up signal is almost straight and the front velocity slows down quickly only close to the maximum run-up level. The velocity records in Figures 5.7-5.9 show often a certain duration where the velocity is quite close to the maximum velocity (which is always a little peaked), say within about 20% of the peak value.

For this reason the combined signal of wave run-up and front velocity was judged by eye and three other locations were established from the data. In total the following locations where derived, see also Figure 5.10.

| | |
|---|---|
| $R_{u\ start}$: | the location where the run-down changes into run-up |
| $R_{u\ min}$ at ~$u_{max}$: | the lowest location where the velocity is within about 20% of its maximum velocity |
| $R_u$ at $u_{max}$: | the location where umax has been calculated (data processing) |
| $R_{u\ max}$ at ~$u_{max}$: | the highest location where the velocity is within about 20% of its maximum velocity |
| $R_{u\ max}$: | the maximum run-up level (data processing) |

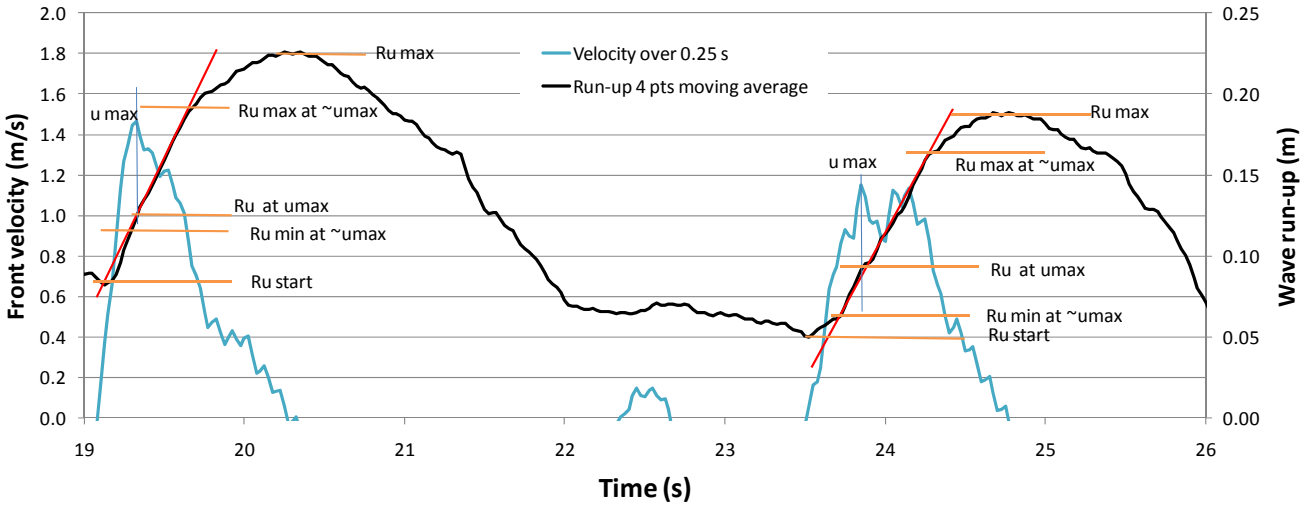


Figure 5.10. Two waves of test 456 with definition of five run-up levels.

First the analysis of calculated maximum velocity, $u_{max}$, will be compared with the maximum run-up of that wave, $R_{umax}$, and with the location with respect to the run-up, $R_{umax}$ - $R_u$ at $u_{max}$. Then the five different run-up levels as defined above will be compared with each other.

Figure 5.11 shows $u_{max}$ versus $R_{u\ max}$ in the same wave, for tests 148 en 149 (slope 1:3) and for velocities larger than about 1 m/s. There is a large scatter. Although the run-up values in average are smaller for test 149, the velocities seem to be more or less similar.

Figure 5.12 shows $u_{max}$ versus the location on the slope where this $u_{max}$ was found. As described above, to be able to calculate a reliable velocity the velocity record had to be averaged over a certain short time. This means that de location where $u_{max}$ was calculated, would be somewhere on the slope covered in that short period. Depending on the velocity the actual location could be a little lower than given in Figure 5.12. The straight line in the graph, compared to the vertical axis, shows the distance the front of the wave can travel in that short time. Most of the data points are close to the water level, but certainly above it, and a significant part shows maximum velocities well above the still water level.

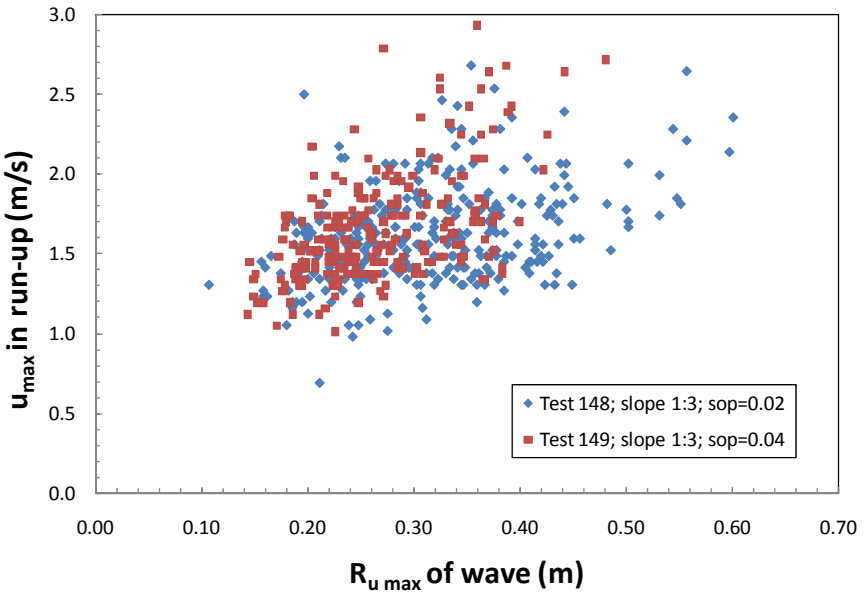


Figure 5.11. Maximum velocity versus maximum run-up level. Tests on 1:3 slope.

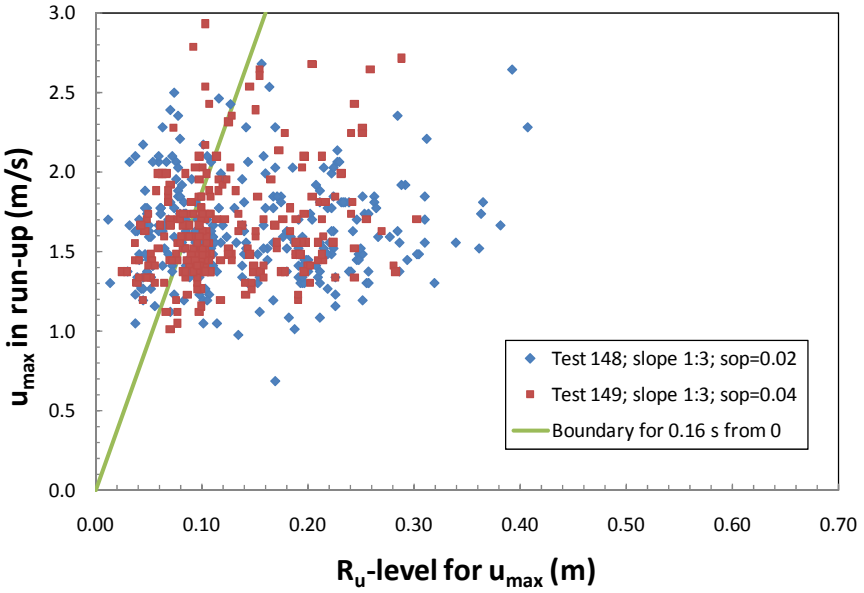


Figure 5.12. Maximum velocity versus location on the slope. Tests on 1:3 slope.

Figure 5.13 shows the maximum velocity versus the distance between the maximum run-up in that wave and the location where the maximum velocity was found: $R_{umax}$ - $R_u$ at $u_{max}$. The assumption in Chapter 4 was that the following relationship would be present:

$$u = c_u [ g(R_u - R)]^{0.5} \quad (5.1)$$

For u and $R_u$ the 2%-level was taken and the coefficient found was close to $c_{u\ 2\%}$ = 1.4. In the present analysis we have velocities and maximum run-up correlated, which gives the following similar equation, but now for each wave:

$$u_{max} = c_u [ g(R_{u\ max} - R_u\text{-level for } u_{max})]^{0.5} \quad (5.2)$$

Figure 5.13 shows the data points with Equation 5.2. Note that the graph gives only the data for velocities larger than 1 - 1.5 m/s and that there will be many data points for smaller velocities, but these have not been analyzed. Also the test with smaller wave height, 146, has been given.

The overall conclusion is that there is a large scatter for individual waves, but the relationship 5.2, with a coefficient $c_u$ = 1.4, seems to describe the average trend.

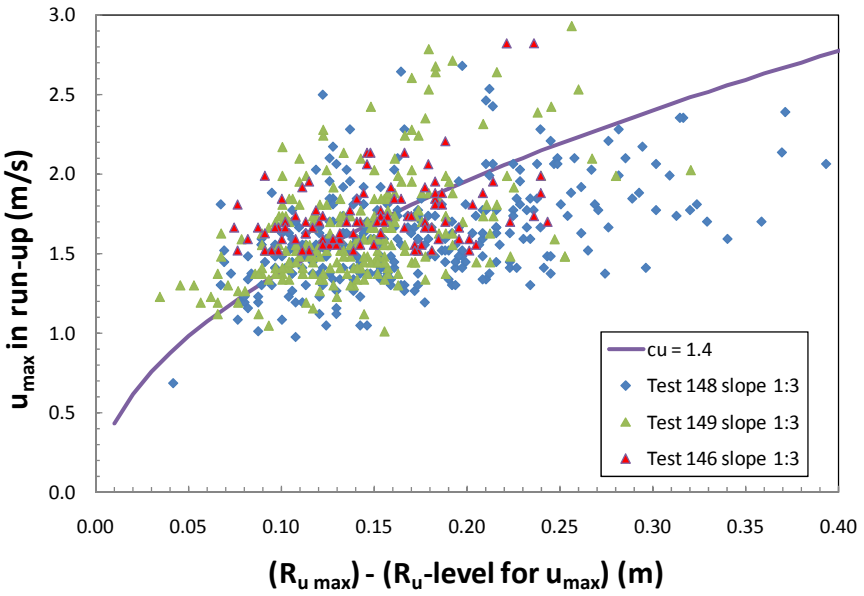


Figure 5.13. Maximum velocity versus relative location on the slope; tests on 1:3 slope.

Tests 146 and 148 are "scale tests" of each other, where test 148 was performed with a 1.5 larger wave height (and similar wave steepness). The relative 2%-run-up values were almost identical, see Figure 5.3. Figure 5.14 shows the dimensionless maximum velocities versus the dimensionless maximum run-up of the same wave. Data was limited to $u_{max}/(gH_s)^{0.5}$ > 1.5 to make both tests comparable. The two clouds of data points cover each other quite well, except for two high outliers for test 146.

The conclusion is that the two tests show quite well identical dimensionless results, with respect to run-up as well as maximum velocity on the slope.

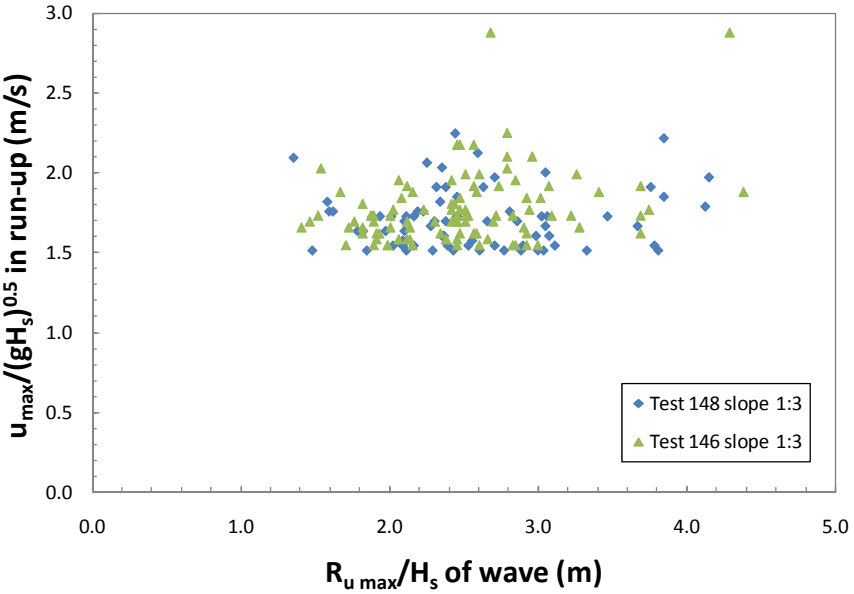


Figure 5.14. Comparison of tests 146 and 148 (scale tests) on maximum velocity.

Figures 5.15 - 5.17 are similar to Figures 5.11 - 5.13, but give now tests 456 and 457 for the gentler slope 1:6. Figure 5.15 shows that smaller run-up values also lead to smaller maximum velocities, which is different from the 1:3 slope, see Figure 5.11.The same conclusion can be drawn for the location of the maximum velocity on the slope, see Figure 5.16: a lot of data points are close to, but above, the still water level, where a significant part of the data is well above the still water level.

Also Figure 5.17 leads to a similar conclusion as for Figure 5.13: that there is a large scatter for individual waves, but relationship 5.2, with a coefficient $c_u$ = 1.4, seems to describe the average trend.

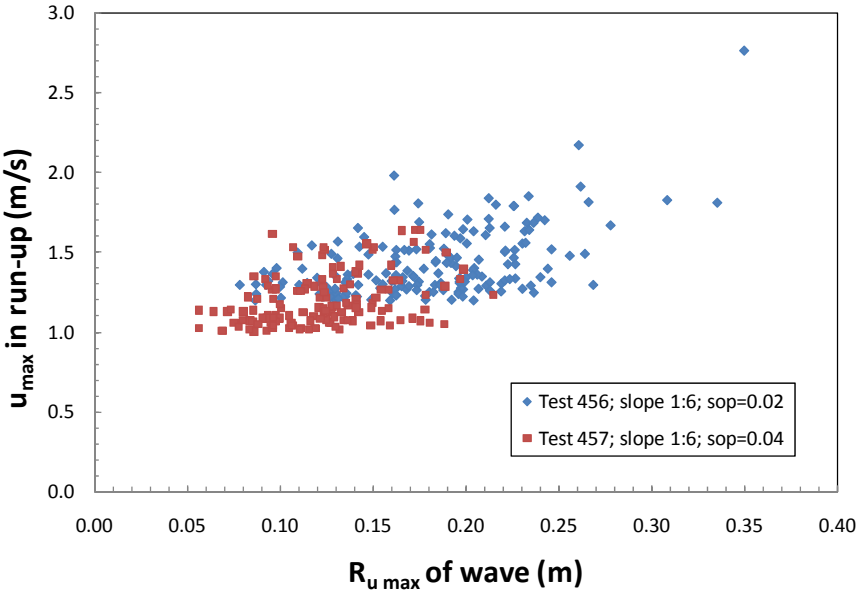


Figure 5.15. Maximum velocity versus maximum run-up level. Tests on 1:6 slope.

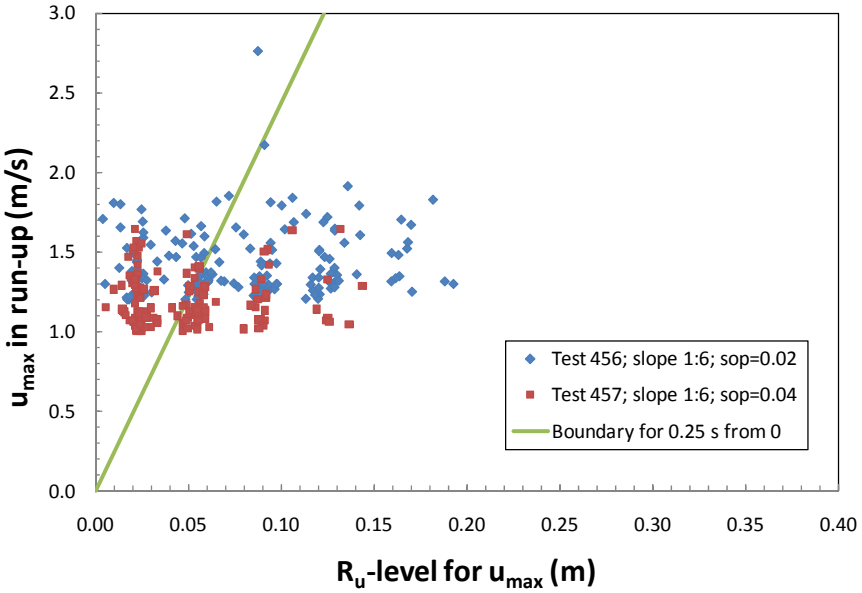


Figure 5.16. Maximum velocity versus location on the slope. Tests on 1:6 slope.

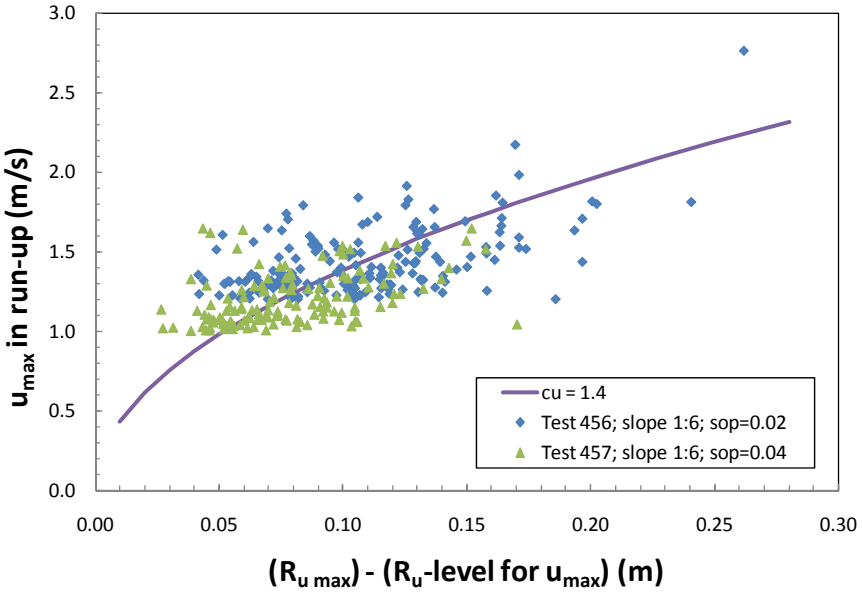


Figure 5.17. Maximum velocity versus relative location on the slope; tests on 1:6 slope.

As more or less similar conclusions were drawn for the 1:3 as well as the 1:6 slope, the data can be combined. Figure 5.18 shows the dimensionless maximum velocity versus the relative location on the slope, with equation 5.2. All data clouds follow the given relationship, but the scatter for individual waves is large.

This aspect has not been described in earlier research. There is a similarity with the distribution of wave heights and wave periods in a sea state. There are small individual wave heights with small wave periods, but also with larger periods. There is a trend between individual wave heights and wave periods, but not a direct relationship. And that seems similar for maximum velocities and the location on the slope where this velocity occurs.

As the scatter is quite large, it may also be useful to look at a relationship between the maximum velocity and the individual maximum run-up. Figure 5.19 shows this relationship. It shows a very similar picture as in Figure 5.18. The coefficient used in

Equation 5.2 is now $c_u$ = 1.0. Comparison of the two graphs leads to a surprising conclusion: the location where the maximum velocity is found, is far from trivial. It is not true that the maximum velocity is found at the water level and that this velocity decreases more or less linearly when the wave rushes up the slope. If that would have been true, than Figure 5.18 would have shown much less scatter than Figure 5.19. The location on the slope where the velocity is maximum is highly variable and a relationship with the individual maximum run-up seems as good as a relationship with the relative difference.

Figures 5.20 and 5.21 give similar graphs as in Figures 5.18 and 5.19, but the data are now given in real values, not in dimensionless terms. As only test 146 has a smaller wave height, this data group is located at a different area, but of course still around the given relationship.

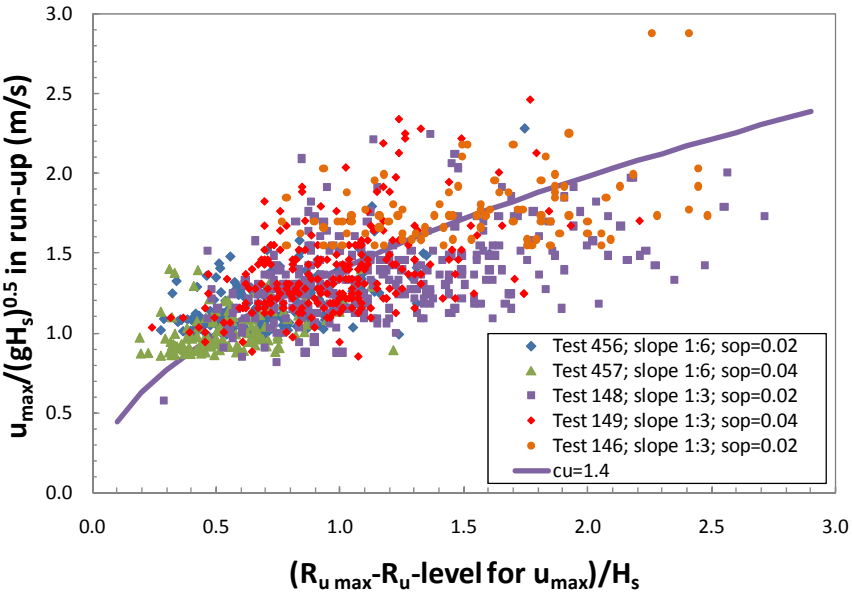


Figure 5.18. Relative maximum velocity versus relative location on the slope; all tests.

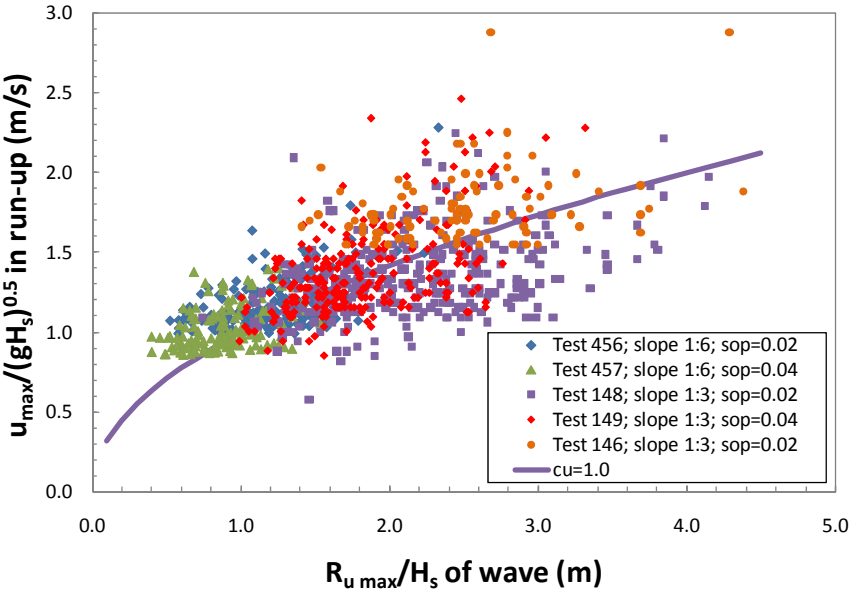


Figure 5.19. Relative maximum velocity versus relative run-up on the slope; all tests.

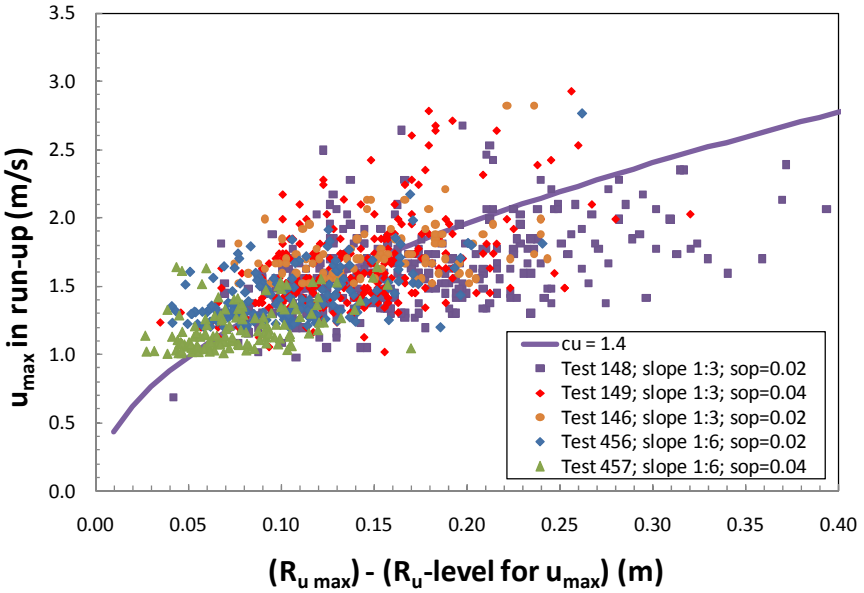


Figure 5.20. Maximum velocity versus location on the slope; all tests.

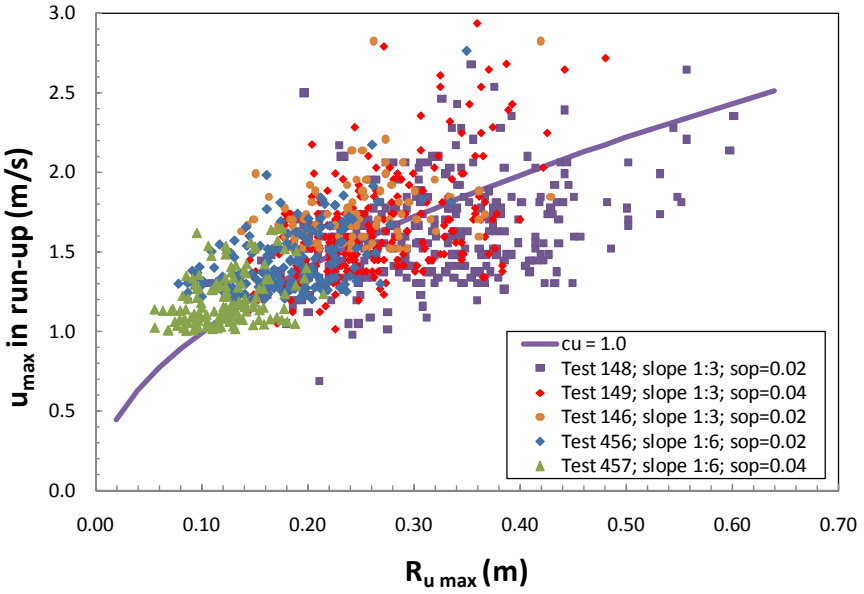


Figure 5.21. Maximum velocity versus run-up on the slope; all tests.

Figures 5.22 - 5.24 give the results for the measurements during a storm at 9 November 2007 at the Petten Seadike. Figures 5.2, 5.6 and 5.9 were described earlier and show the run-up location, part of the measured run-up record and part of the calculated velocity record. The run-up gauge started about 3 m above the storm surge level, which means that not all up-rushing waves reached this gauge. Moreover, the dike profile has an 11 m long berm about 2.5 m above the storm surge level, which makes it difficult to compare the results with other slope angles. As the run-up gauges starts above the storm surge or still water level, it is also not possible to calculate the maximum velocity for the whole slope (with berm) above swl, only for the part on the upper slope, where the gauge was present.

Figure 5.22 shows the maximum velocity on the upper slope versus the maximum run-up of that wave. Only velocities exceeding 2 m/s were evaluated. There seems to be a clear trend that a larger run-up gives a larger velocity. Figure 5.23 shows the same maximum velocities, but now versus the location on the upper slope where this velocity was found. Note that a run-up level of 3 m is about the start of the run-up

gauge. The majority of the points is quite close to this lower level, but a significant part shows the maximum velocity much higher up the slope. This conclusion is similar to the one for the Flowdike slopes.

Figure 5.24 shows the maximum velocity versus the distance between the maximum run-up in that wave and the location where the maximum velocity was found: $R_{umax}$ - $R_u$ at $u_{max}$. Also Equation 5.2 is given with $c_u$ = 1.4. The majority of the points is below the curve, which may be explained by the fact that maximum velocities were only calculated on the upper slope, starting 3 m above swl. Larger velocities have certainly been present on the part between swl and the run-up gauge.

Although a direct comparison with the Flowdike tests is not possible, the analysis shows again that the maximum velocity is not always on the lower part of the slope, but sometimes quite close to the maximum run-up level.

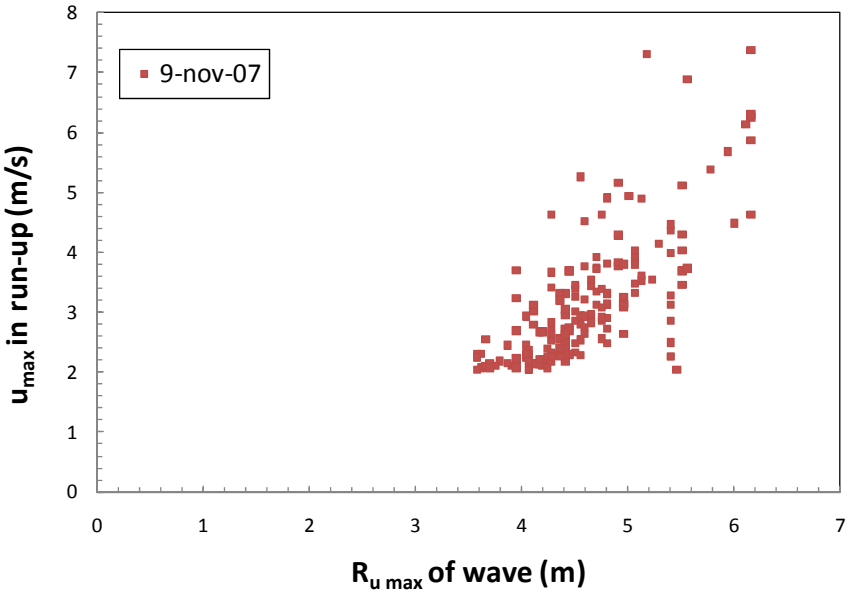


Figure 5.22. Maximum velocity versus maximum run-up level. Tests at Petten Seadike, 9 November 2007.

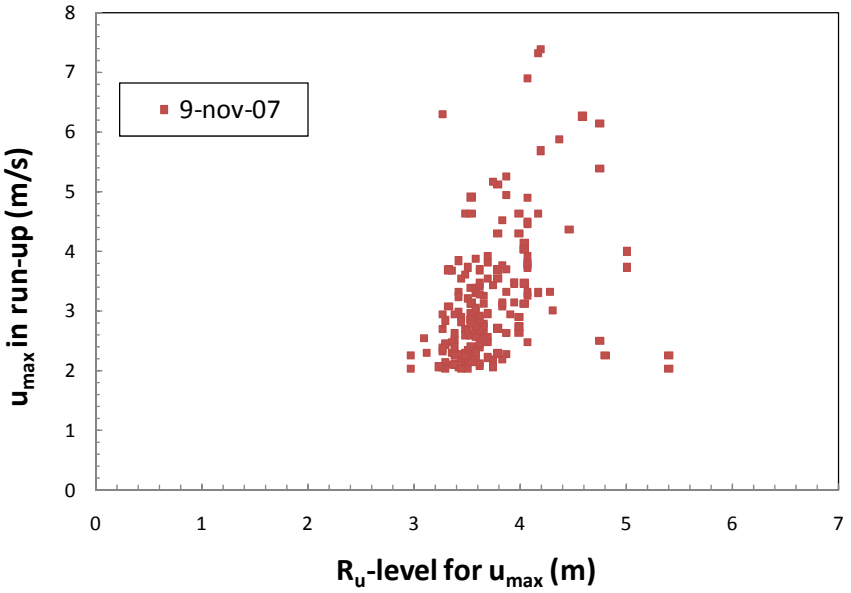


Figure 5.23. Maximum velocity versus location on the slope. Tests at Petten Seadike, 9 November 2007.

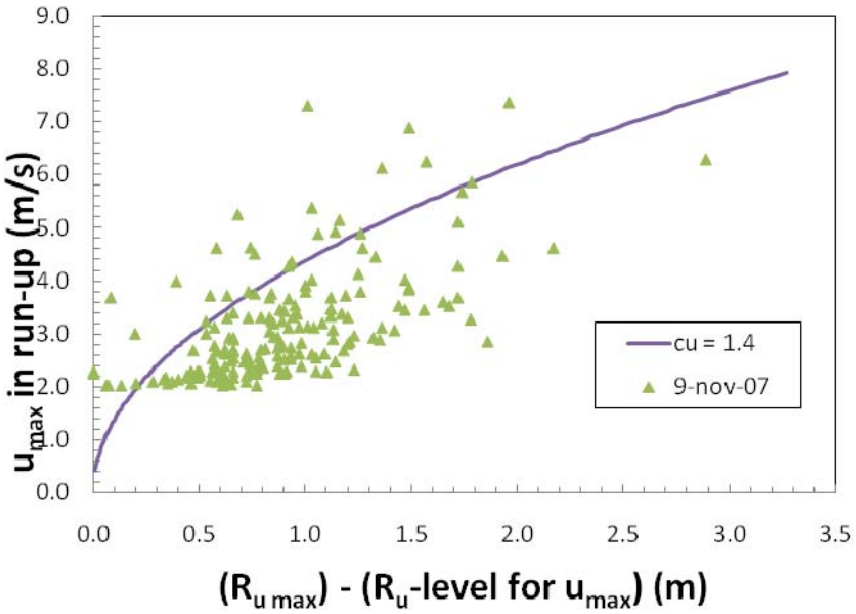


Figure 5.24. Maximum velocity versus relative location on the slope; Tests at Petten Seadike, 9 November 2007.

## 5.3 Analysis of various run-up levels in the run-up zone

Figure 5.10 showed the record of two up-rushing waves and five different levels of run-up have been defined. The location of the maximum velocity and the maximum run-up were discussed above. Figure 5.10, however, also shows where run-down turns into run-up and the two boundaries where between the velocity seems to be constant and quite close to the maximum velocity (given as a straight line along part of the run-up record).

These five run-up levels have been compared in Figures 5.25 and 5.26. Each analyzed wave is given in the graph in ascending order with respect to the maximum run-up level. Figure 5.25 gives test 148 on a 1:3 slope for a steepness of $s_{op}$ = 0.02. The maximum run-up level covers the range from 0.2 - 0.6 m. The 2%-run-up level is given too, which makes it easy to find the waves that exceeded this level. The bold lines give the upper and lower boundaries where the velocity is large and close to the maximum velocity. A number of conclusions can be drawn from the graph.

There is not much difference between where the run-up starts and the minimum run-up level where the velocity is close to the maximum velocity: the two bold lines on the lower part of the graph are almost identical. These two lines also show that run-up does often start at a higher point than the still water level: the up-rushing wave reaches the down-rush of the previous wave before the run-down has reached the still water level.

The other bold line for the upper boundary where the velocity is still close to the maximum velocity, is always quite close to the maximum run-up level. This leads to the conclusion that a large velocity, close to the maximum velocity, is present from the start of run-up to a high level close to the maximum run-up.

The maximum run-up in average is found closer to the lower boundary than the upper boundary. Figure 5.25 also shows that for run-up levels exceeding the 2%-value, the run-up starts well above swl and the location of the maximum velocity is quite high on the slope.

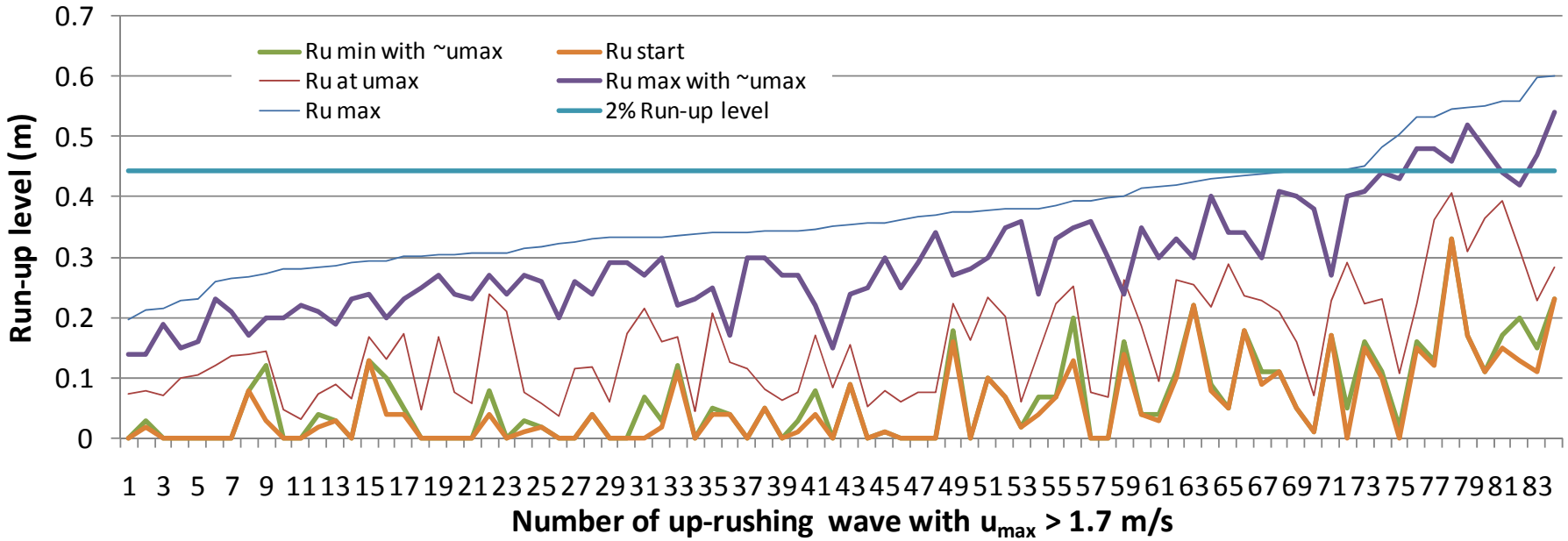


Figure 5.25. Various run-up levels in ascending order. Test 148, slope 1:3.

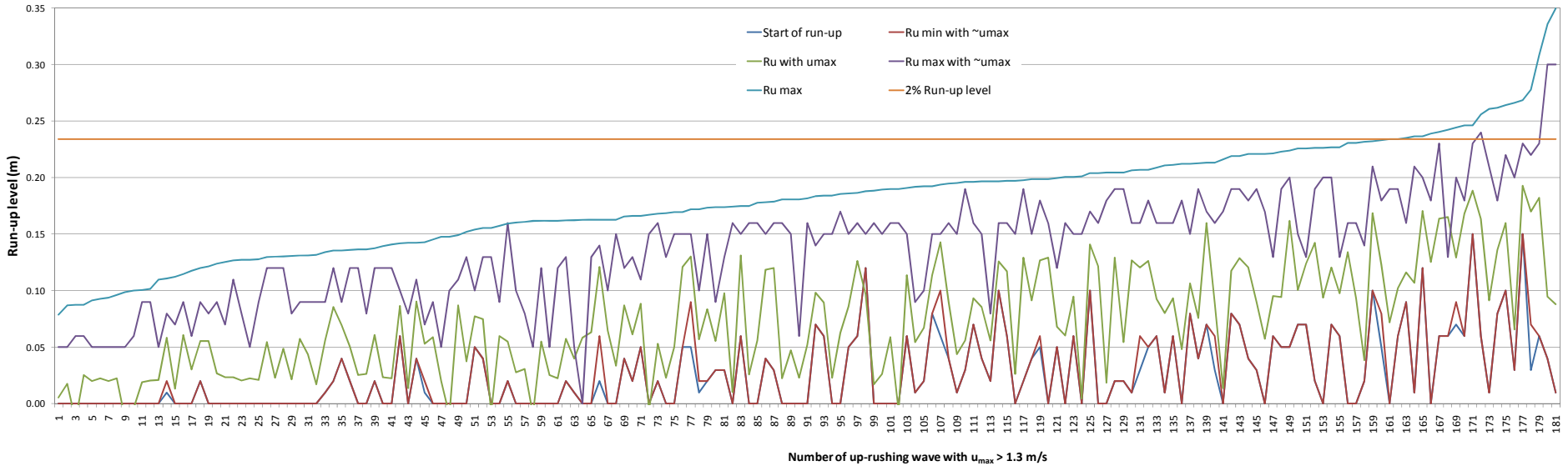


Figure 5.26. Various run-up levels in ascending order. Test 456, slope 1:6.

Figure 5.26 gives the data of test 456 on a 1:6 slope, again with a wave steepness of $s_{op}$ = 0.02. The wave run-up levels have now been covered between 0.08 m and 0.35 m. The similarity between the start of run-up and the lower boundary is even better than for test 148 in Figure 5.25. Similar conclusions can be drawn for the maximum boundary and for the level of maximum velocity. Actually, a slope of 1:3 and 1:6 give the same conclusions.

From both graphs some statistical values may be calculated, which may help to formulate more concise conclusions. If all levels are compared to the maximum run-up of the wave considered, a relative level is reached. Tests 148 and 456 gave an average level of respectively 15% and 14% for the lower boundary where the velocity is still close to the maximum velocity. This level is almost equal to where wave run-up starts. The location for the maximum velocity in average is found for levels of 41% and 38%, respectively. The average levels for the maximum boundary where the velocity is still close to the maximum velocity, were found at 78% and 74%, respectively.

The various values for the two slopes are quite similar. This leads to the following conclusion on the location of maximum or large velocities in the run-up of waves on the seaward slope of a smooth dike:

**In average the run-up starts at a level of 15% of the maximum run-up level, with a velocity close to the maximum velocity and this velocity is more or less constant until a level of 75% of the maximum run-up level. The real maximum velocity in average is reached between 30%-40% of the maximum run-up level.**

Above conclusion explains for a part why the relationship between the maximum velocity and the location on the slope with respect to the maximum run-up (see Figure 5.18) gives a lot of scatter. A velocity close to the maximum velocity is present over a large part of the slope and the actual location of the maximum velocity may be more or less "by accident". As Figure 5.18 and 5.19 show similar scatter, there is a good reason to use above conclusion and Figure 5.19 as a reference to calculate maximum velocities.

Figure 5.19 has been repeated in Figure 5.27, but now with curves with different values for the coefficient $c_u$ of 0.6 and 0.8 (below the middle curve) and 1.2 and 1.4 (above the middle curve). Note that for velocities of $u_{max}/(gH_s)^{0.5} < 1$ data has not been evaluated, but will be there in reality. Looking at the upper curve about 10% of the points above the middle curve will even be larger than this curve. This suggests that the upper curve (and also the lower curve) could be considered as 90% confidence levels. Assuming a normal distribution of the velocities around the average value (the middle curve) leads to a variation coefficient of V = (1.4 - 1.0)/1.64 = 0.24. This value could be rounded of to 0.25.

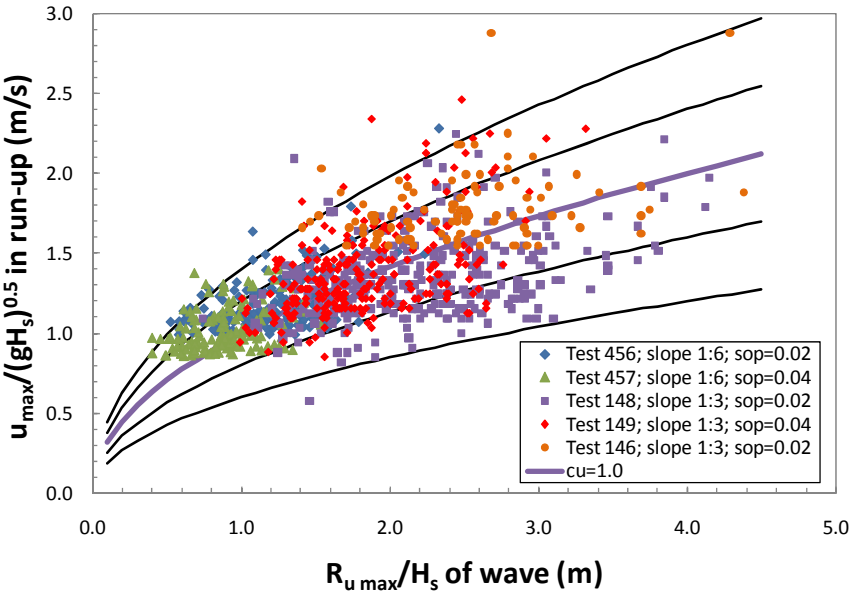


Figure 5.27. Relative maximum velocity versus relative wave run-up, including uncertainty levels.

**The conclusion may then be that the maximum velocity on a slope can be calculated by:**

$$u_{max}/(gH_s)^{0.5} = c_u\,(R_{u\,max}/H_s)^{0.5} \qquad (4.14)$$

**with $c_u$ as stochastic variable with $\mu(c_u) = 1.0$ and a normal distribution with V = 0.25.**

## 5.4 Distributions of run-up and velocity

The analysis on maximum velocities and run-up levels can be used to make exceedance curves and compare them with a Rayleigh distribution. This comparison is easy if the horizontal scale is according to a Rayleigh scale. For such a graph a measured distribution is close to a Rayleigh distribution if the curve is close to a straight line in the graph. First the run-up distributions will be described and then the velocity distributions.

Figures 5.28-5.30 show the run-up distributions for tests 146, 148 en 146; 456 and 457; and finally for the measurements at the Petten Seadike. It should be noted that the run-up values were not established in a direct way. Maximum velocities were analyzed above a certain threshold, together with the maximum run-up for that wave. Large run-up values, but with velocities smaller than the threshold, were not taken into account. This is the reason in the graphs that the lower part turns downwards. In all cases in Figures 5.28-5.30 the upper part of the curves could be considered as fairly straight, although this conclusion could be stronger if more run-up values would have been taken into account.

Figures 5.31-5.32 show the velocity distributions for velocities exceeding a certain value. In all cases the curves are fairly straight, leading to the conclusion that also velocity distributions might be according to a Rayleigh distribution.

Conclusions above on velocity are similar to the conclusions given in Section 4.5 and Figure 4.18.

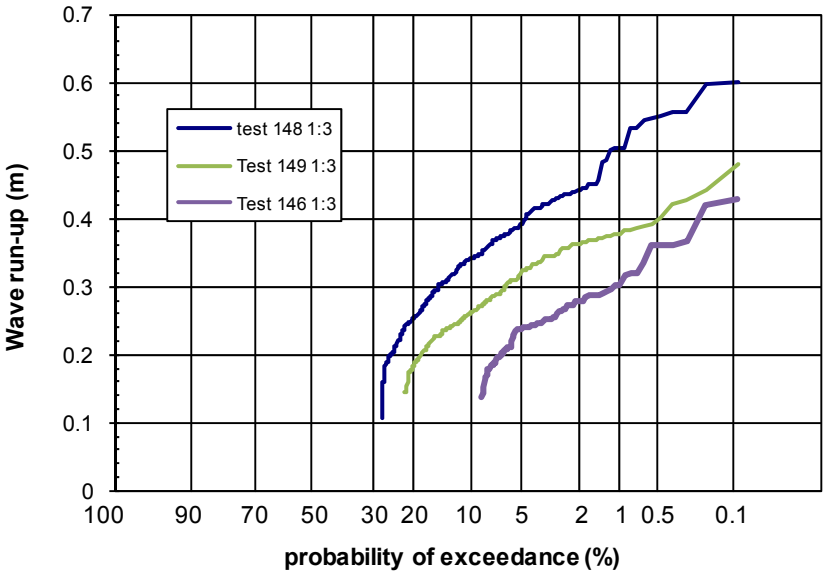


Figure 5.28. Run-up distributions for tests 146, 148 and 149.

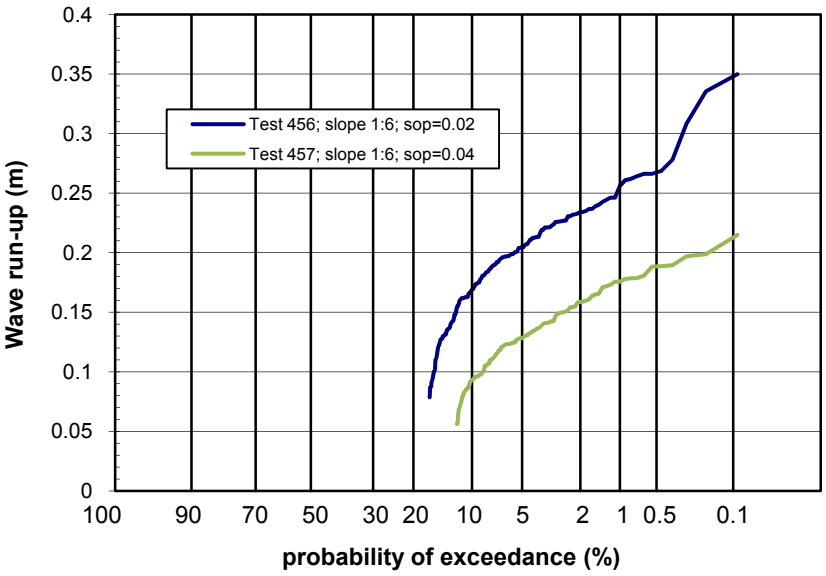


Figure 5.29. Run-up distributions for tests 456 and 457.

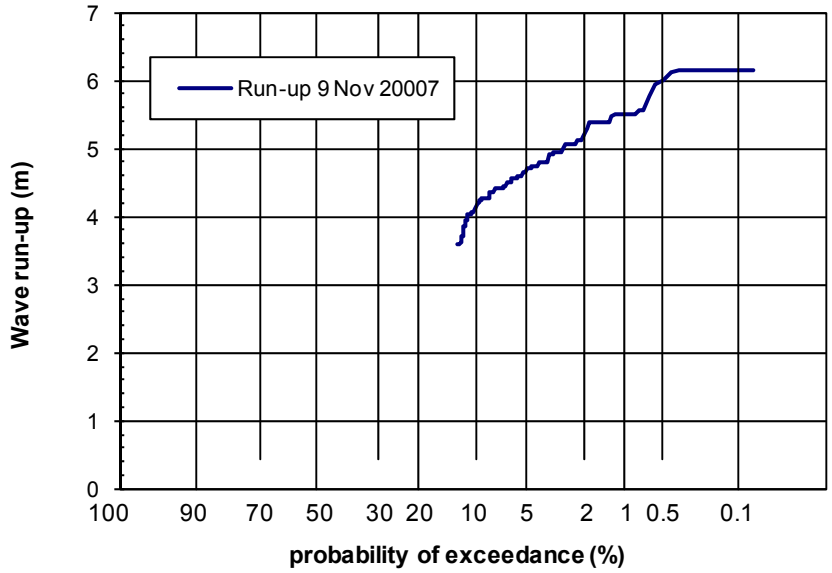


Figure 5.30. Run-up distribution for measurements at the Petten Seadike.

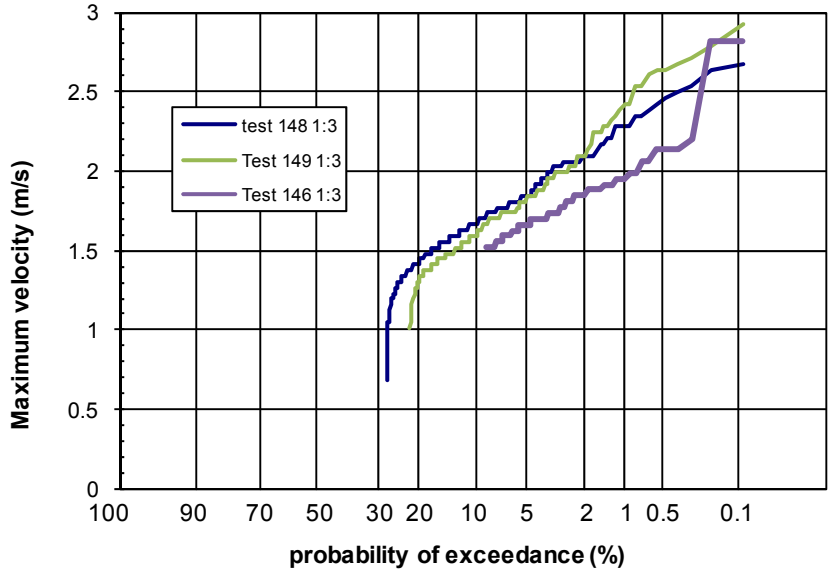


Figure 5.31. Velocity distributions for tests 146, 148 and 149.

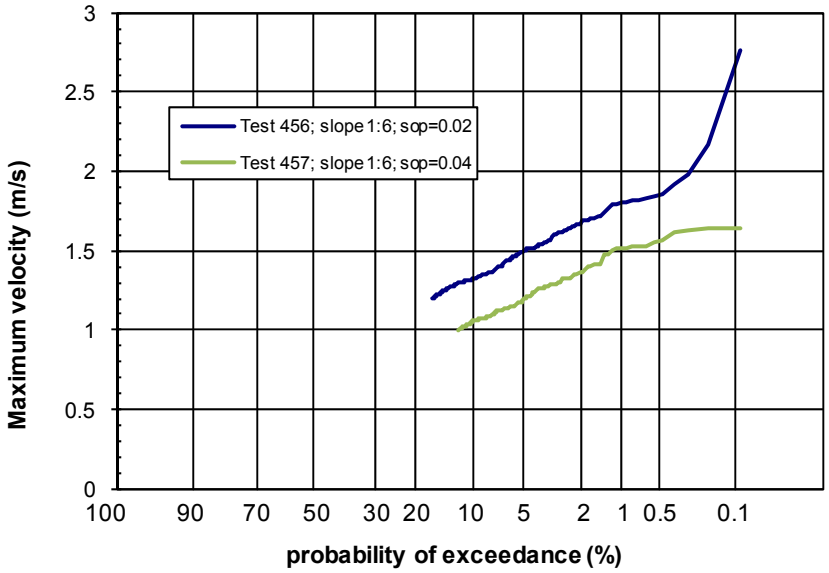


Figure 5.32. Velocity distributions for tests 456 and 457.

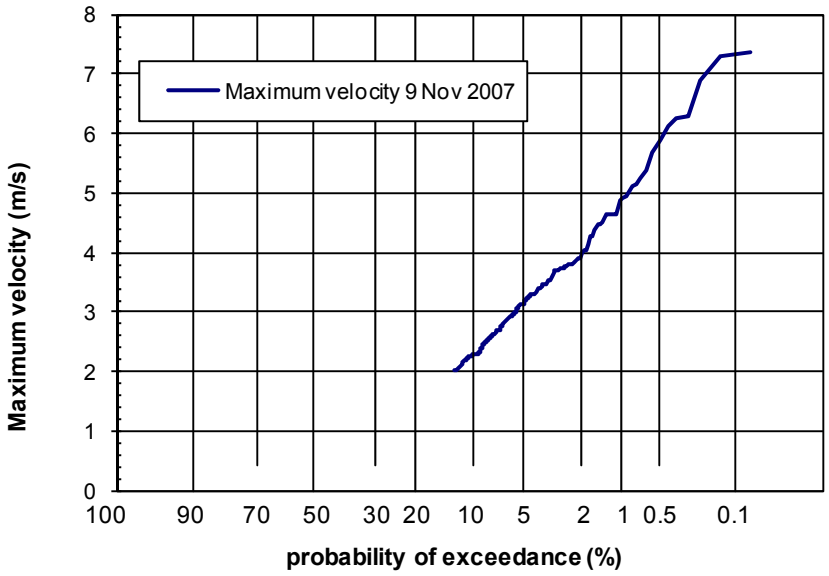


Figure 5.33. Velocity distribution for measurements at the Petten Seadike.

# 6 Design of the Wave Run-up Simulator

The Wave Run-up Simulator will be quite similar to the Wave Overtopping Simulator, but with a number of modifications. The Wave Run-up Simulator should simulate up-rushing waves on a slope with correct velocities and giving correct run-up levels. This is different from the Wave Overtopping Simulator, which is based on simulating correct velocities for given overtopping wave volumes. Also different velocities should be simulated for similar run-up levels, simulating the scatter that is present in the graphs with velocity versus run-up. Another problem to solve is that the up-rushing waves come back as rundown to the Simulator. The water has to be released before the next up-rushing wave will be simulated.

What the Wave Run-up Simulator should simulate can be taken from the conclusions of the analyses in Chapters 4 and 5.

In average the run-up starts at a level of 15% of the maximum run-up level, with a velocity close to the maximum velocity and this velocity is more or less constant until a level of 75% of the maximum run-up level. The real maximum velocity in average is reached between 30%-40% of the maximum run-up level.

The maximum velocity on a seaward slope can be calculated by:

$$u_{max}/(gH_s)^{0.5} = c_u\ (R_{u\ max}/H_s)^{0.5} \qquad (4.14)$$

with $c_u$ as stochastic variable with $\mu(c_u) = 1.0$ and a normal distribution with $V = 0.25$.

The flow depth remains a parameter where no concise conclusion can be given. But it is a parameter that does not show up in the cumulative overload method, and therefore, could be considered as less important. Chapter 4 comes to the following conclusion on flow depth:

A conclusion could be to take $c_{h2\%} = 0.20$ for slopes of 1:3 and 1:4 and $c_{h2\%} = 0.30$ for a slope of 1:6. Consequently, a slope of 1:5 would then by interpolation give $c_{h2\%} = 0.25$. This procedure is better than to use a formula like $c_{h2\%} = 0.055\ \cot\alpha$, as given in EurOtop (2007).

The 2% wave run-up levels can be calculated according to the EurOtop Manual (2007) and a Rayleigh distribution can be assumed to calculate other run-up levels.

The cumulative overload method can directly be applied to the grass cover on the seaward slope, using the equations and methods described above.

The mechanical design has to solve the problem of simulating different velocities for similar run-up levels and the fact that water comes back by run-down. The first problem can probably be solved by the method that has been developed for the US Simulator. In that case different flow times of overtopping wave volumes had to be simulated, for similar volumes. A long wave period would give a longer flow time than a short period, for the same overtopping wave volume. The solution was to control the opening size of the valve. A full opening would give the shortest flow time, a more closed opening would give longer flow times. This method appeared to work well (the opening of the valve can be steered to 1 degree accuracy). A similar method can also solve the problem of simulating different velocities for similar run-up levels.

The problem that water returns by down-rush can be solved by modifying the transition from the box of the Simulator to the slope to a movable one. If space is created for rundown to be released (moving up the transition or opening a valve) the problem will be solved.

With the description of wave run-up as given above and the possible solutions to be developed to simulate run-up in a correct way, it must be possible to develop a Wave Run-up Simulator without large investment or time needed to come to a properly working machine.

## References


Akkerman, G.J., P. Bernardini, J.W. van der Meer, H. Verheij and A. van Hoven 2007). Field tests on sea defineces subject to wave overtopping. *Proc. Coastal Structures, Venice, Italy.*

Bosman, G, J.W. van der Meer, G. Hoffmans, H. Schüttrumpf and H.J. Verhagen. 2008. Individual overtopping events at dikes. *ASCE, proc. ICCE 2008, Hamburg, Germany, p. 2944-2956*.

Dean, R.G., J.D. Rosati, T.L. Walton and B.L. Edge (2010). Erosional equivalences of levees: Steady and intermittent wave overtopping. *Journal of Ocean Engineering 37 (2010) 104-113.*

EurOtop Manual. 2007. Wave Overtopping of Sea Defences and Related Structures – Assessment Manual. UK: N.W.H. Allsop, T. Pullen, T. Bruce. NL: J.W. van der Meer. DE: H. Schüttrumpf, A. Kortenhaus. www.overtopping-manual.com.

Hoffmans, G., G.J. Akkerman, H. Verheij, A. van Hoven and J.W. van der Meer (2008). The erodibility of grassed inner dike slopes against wave overtopping. *ASCE, Proc. ICCE 2008, Hamburg, 3224-3236*.

Le Hai Trung, J.W. van der Meer, G.J. Schiereck, Vu Minh Cath and G. van der Meer (2010). Wave Overtopping Simulator Tests in Vietnam. ASCE, *Proc. ICCE 2010, Shanghai.*

Lorke, S., A. Brüning, J.W. van der Meer, H. Schüttrumpf, A. Bornschein, S. Gilli, R. Pohl, M. Spano, J. Riha, S. Werk and F. Schlütter. On the effect of current on wave run-up and wave overtopping. *ASCE, Proc. ICCE 2010, Shanghai.*

Schüttrumpf H. and H. Oumeraci (2005). Layer thicknesses and velocities of wave overtopping flow at seadikes. *Journal of Coastal Engineering, Volume 52, Issue 6, p. 473-495.*

Schüttrumpf, H. and M.R.A. van Gent, 2003. Wave overtopping at seadikes. *ASCE, proc. Coastal Structures 2003, p. 431-443.*

Schüttrumpf, H.F.R. 2001. Wellenüberlaufströmung bei See-deichen, *Ph.D.-thesis, Technical University Braunschweig.*

Steendam, G.J., W. de Vries, J.W. van der Meer, A. van Hoven, G. de Raat and J.Y. Frissel (2008). Influence of management and maintenance on erosive impact of wave overtopping on grass covered slopes of dikes; Tests. *Proc. FloodRisk, Oxford, UK. Flood Risk Management: Research and Practice – Samuels et al. (eds.) ISBN 978-0-415-48507-4; pp 523-533.*

Steendam, G.J., J.W. van der Meer, B. Hardeman and A. van Hoven (2010). Destructive wave overtopping tests on grass covered landward slopes of dikes and transitions to berms. *ASCE, Proc. ICCE 2010, Shanghai*.

Van der Meer, J.W., P. Bernardini, W. Snijders and H.J. Regeling (2006). The wave overtopping simulator. *ASCE, ICCE 2006, San Diego, pp. 4654 - 4666*.

Van der Meer, J.W., P. Bernardini, G.J. Steendam, G.J. Akkerman and G.J.C.M. Hoffmans (2007). The wave overtopping simulator in action. *Proc. Coastal Structures, Venice, Italy.*

Van der Meer, J.W., G.J. Steendam, G. de Raat and P. Bernardini (2008). Further developments on the wave overtopping simulator. *ASCE, Proc. ICCE 2008, Hamburg, 2957-2969.*

Van der Meer, J.W., R. Schrijver, B. Hardeman, A. van Hoven, H. Verheij and G.J. Steendam (2009). Guidance on erosion resistance of inner slopes of dikes from three years of testing with the Wave Overtopping Simulator. *Proc. ICE, Coasts, Marine Structures and Breakwaters 2009, Edinburgh, UK.*

Van der Meer, J.W., B. Hardeman, G.J. Steendam, H. Schttrumpf and H. Verheij (2010). Flow depths and velocities at crest and inner slope of a dike, in theory and with the Wave Overtopping Simulator. *ASCE, Proc. ICCE 2010, Shanghai*.

Van Gent, M.R.A. 2002. Low-exceedance wave overtopping events. *Delft Hydraulics project id. DC030202/H3803.*

Van Hoven, A., B. Hardeman, J.W. van der Meer and G.J. Steendam (2010). Sliding stability of landward slope clay cover layers of sea dikes subject to wave overtopping. *ASCE, Proc. ICCE 2010, Shanghai.*